

POLITECNICO DI MILANO
School of industrial and information Engineering
Master's Degree in Nuclear Engineering



**Methods for characterization of X ray imaging
systems performance using Modulation
Transfer Function in industrial applications:
Focal Spot, Magnification and Physical
Filtering analysis**

Politecnico di Milano
collaboration with Gilardoni S.P.A.

Supervisor: Prof. Marco Caresana
Co-Supervisor: Ing. Davide Baratto

Candidate:
Riccardo Maria Zito
Code 945887

Academic Year 2020-2021

*For a successful technology, reality must take precedence over
public relations, for nature cannot be fooled.*

Richard P. Feynman

Abstract

Modulation Transfer Function, or MTF, is an image quality indicator, that provides the contrast degradation due to the imaging system, including objects, detector and electronics. In this thesis, MTF measures performed with the IQI EN 462-5 are exploited to analyze the system itself, and then the features of the industrial applications of physical filters. First, the system, the Cabinet XE-L HE by Gilardoni S.P.A., was calibrated, correcting bad pixels, dark current and gain, along with the implementation of a program in Matlab for the computation of the Lag.

After that, the effects of the parameters of the system on the MTF are analyzed, and so it is done for the "Ratio method" presented below, looking also for stationary points, so that they can provide more stability to the MTF with respect to parameters fluctuations not expected.

Then, two methods are presented, used to characterize the focal spot dimension, the first one, called here "Ratio method" is fast and quite simple, the second one, called here "Optimal magnification method", requires a little more time in order to identify the magnification providing the maximum MTF value as a function of the focal spot, but it provides precise measures of focal spot dimension and useful insights on the behavior of MTF at different distance from the source. The examples reported in the thesis show that the nominal value is enclosed within 1 coverage factor for the 1 mm focal spot, and within a coverage factor of 2 for the 0.4 mm focal spot. Then, this method is used also to measure the effect of filtration at source on the equivalent focal spot dimension.

Then, it is performed the analysis of the effects of filtration according to MTF. To compare different MTFs, it was used a particular value of spatial frequency, namely the ones reducing the MTF to 10% or 5%, depending on the application discussed. It is demonstrated their equivalency in terms of parameters of the system. Then, applications of filters to radiology and extendable to tomography were analyzed, studying brass filters with water, aluminum and iron objects.

Abstract

Modulation Transfer Function, o MTF, è un indicatore di qualità immagine, il quale fornisce la degradazione del contrasto dovuto al sistema di imaging, compresi oggetti, detector e l'elettronica. In questa tesi, le misure di MTF, effettuate con l'IQI EN 462-5 sono state utilizzate per analizzare il sistema stesso e successivamente le caratteristiche per applicazioni industriali dei filtri fisici. Inizialmente, il sistema, cioè la Cabina XE-L HE di Gilardoni S.P.A, è stata calibrata, correggendo i bad pixels, corrente di buio e gain, insieme con l'implementazione di un programma in Matlab per il calcolo del Lag.

Dopo questo, l'effetto dei parametri sull'MTF è stato analizzato, e lo stesso è stato fatto per il "metodo del rapporto" presentato oltre, con lo scopo di cercare punti stazionari, cosicché essi potessero fornire maggiore stabilità all'MTF rispetto a fluttuazioni non previste dei parametri.

Successivamente, vengono presentati due metodi, usati per caratterizzare la dimensione della macchia focale, il primo chiamato "metodo del rapporto" è rapido e abbastanza semplice, il secondo, chiamato qui "metodo della magnificazione ottima", richiede maggior tempo per identificare l'ingrandimento che fornisce il massimo MTF in funzione della macchia focale, ma fornisce misure precise di dimensione di macchia focale e utili informazioni sul comportamento dell'MTF a differenti distanze dalla sorgente. Gli esempi riportanti nella tesi mostrano che il valore nominale della macchia focale da 1 mm viene compreso con un fattore di copertura pari a 1, mentre per quella da 0.4 mm con un fattore 2. Poi, questo metodo è stato anche utilizzato per misurare l'effetto sulla macchia focale equivalente dell'applicazione di un filtro alla sorgente.

Successivamente è stata effettuata l'analisi degli effetti delle filtrazioni in riferimento all'MTF. Per confrontare diversi MTF, è stato impiegato un particolare valore di frequenza spaziale, quello che riduce l'MTF al 10% o al 5%, a seconda dell'applicazione che è in analisi. In fine, applicazioni radiosopiche, estendibili anche a tomografia, dei filtri sono state valutate, studiando filtri d'ottone con oggetti di acqua, alluminio e ferro.

Estratto

Questo lavoro di tesi ha avuto come obiettivo quello di creare dei metodi per la caratterizzazione del sistema ottico e di utilizzare poi un metodo per produrre delle valutazioni originali in merito ad una tecnologia in utilizzo, le filtrazioni alla sorgente X, al fine di comprenderne vantaggi, svantaggi e limiti di utilizzo, sempre effettuando misure di Modulation Transfer Function, o in breve MTF. La macchina utilizzata è la Cabina XE-L HE by Gilardoni S.P.A., insieme con l'Indicatore Qualità Immagine EN 462-5. In questo caso è un indicatore detto penetrametro a fili, siccome è composto di una serie di coppie di fili di spessore decrescente, distanti quanto il diametro del filo stesso.

Inizialmente vengono introdotti dei brevi richiami di interazione radiazione materia, con riferimento alla radiazione X ed alla tipologia di ragionamento che viene richiesta per questo tipo di analisi.

Successivamente vengono discusse le principali quantità di interesse per la caratterizzazioni della qualità immagini radiografiche, con alcuni cenni alle differenze con quelle tomografiche.

La caratterizzazione del sistema ha visto l'applicazione delle norme dell'ASTM per bad pixels, gain e corrente di buio. L'ipotesi di buona geometria di allineamento ha previsto la valutazione della centratura del fascio rispetto al detector. I piani di rotazione non sono stati caratterizzati siccome in radioscopia rivestono un'importanza marginale. Un lavoro addizionale di calibrazione ha visto la stesura di un programma in Matlab per il calcolo automatico del Lag del sistema. Il Lag è una proprietà del sistema di acquisizione, in particolare del detector, ed è misurato in secondi. Quantifica quanto tempo è necessario attendere, dopo una esposizione ad alta intensità, prima di poter acquisire una nuova immagine che non sia influenzata dall'acquisizione precedente.

Si è poi effettuata un'analisi preliminare del sistema, in modo tale da comprendere eventuali problematiche insite nella strumentazione e impostare il lavoro in modo tale che eventuali caratteristiche non condizionassero i risultati, rendendoli scarsamente ripetibili. Si è poi proseguito con l'analisi della Modulation Transfer Function (MTF). La Modulation Transfer Function è una funzione di trasferimento che collega il contrasto all'ingresso del sistema ottico con quello in uscita da esso. Essa dipende dalle dimensioni di interesse, ed è quindi una funzione delle dimensioni degli oggetti. Siccome in questo campo viene spesso usata l'analisi di Fourier, l'MTF è spesso non come funzione di una dimensione, ma come funzione di una frequenza spaziale, misurata in "coppie di linee per millimetro", [lp/mm]. Lo studio dell'MTF è stato svolto in funzione dei parametri del set-up. Si è confermata una dipendenza della Modulation Transfer Function da mA, kV e magnificazione M. Le dipendenze sono differenti. In particolare, per i mA, l'MTF cresce fino a che non si entra in un regime di saturazione del pannello. Per i kV di tensione, utilizzando solamente l'oggetto di test per la qualità immagine, chiamato Image Quality Indicator (IQI), l'MTF decresce al crescere dei kV. L'andamento dell'MTF in funzione della magnificazione presenta dei massimi locali, che sono di inter-

esse per selezionare posizioni ottime per l'imaging, ed un massimo assoluto, che viene sfruttato nel seguito della tesi per creare una tecnica di analisi della performance del sistema.

Successivamente, l'esigenza di un metodo rapido e semplice, che potesse essere fornito ad un cliente in modo che potesse valutare autonomamente quanto dichiarato dalle schede di specifica e non richiedesse un lavoro lungo e con personale specializzato, ha portato a ideare quello che viene chiamato qui "metodo del rapporto", che viene discusso prima di un secondo metodo, quello con una procedura maggiormente lunga, chiamato "metodo dell'ingrandimento ottimo".

Il metodo del rapporto, così chiamato perché è il rapporto tra le frequenze spaziali che portano al valore del 10% la Modulation Transfer Function di due macchie focali, ha come obiettivo quello di essere utilizzato per caratterizzare la dimensione di una macchia focale rispetto ad una di riferimento e, sfruttando la presenza di punti stazionari del rapporto come funzione di mA e kV, si riesce a creare un metodo che sia stabile anche in assenza di un feedback nei confronti dell'elettronica di potenza.

Il metodo dell'ingrandimento ottimo, invece, richiede maggior tempo, tuttavia fornisce informazioni addizionali molto utili, in particolare gli ingrandimenti dove si hanno punti stazionari della funzione MTF(M), dove M indica la magnificazione del sistema ottico, permettendo quindi di effettuare analisi alla massima risoluzione o di valutare eventuali degradazioni del contrasto dovuti al posizionamento. Per fare confronti tra le diverse curve di MTF viene utilizzato in questa sezione il parametro di frequenza spaziale in [lp/mm] che porta l'MTF al 10%. Durante l'analisi di imaging a spessori elevati, invece, viene utilizzato un MTF al 5%, siccome l'IQI utilizzato presenta frequenze spaziali che possono essere alte in presenza di forte attenuazione.

Questo metodo è stato valutato nella sua precisione andando a misurare le dimensioni di macchia focale o Focal Spot (FS) di due tubi di cui sono note le dimensioni nominali. Per avere conferma della dimensione approssimativa delle macchie sono state effettuate delle misure con il metodo della Slit camera. Le dimensioni sono state calcolate dai risultati di magnificazione ottima, ottenendo come risultati della posizione, per la macchia focale da 1 mm, distanza dal detector di 10 cm contro 9.55 cm calcolati con formule di ottica geometrica, o equivalentemente ingrandimento $M=1.11$ contro $M=1.10$ da calcolo teorico; per la macchia focale da 0.4 mm, distanza di 23 cm rispetto a 21 previsto, o $M=1.28$ rispetto a $M=1.25$ calcolato. Tramite una stima di errore nel posizionamento di 1 cm per la macchia focale da 1 mm e 1.5 cm per la macchia focale da 0.4 mm, dovuta a diversa stabilità dell'operatore nella misura, tramite la formula di propagazione delle incertezze, si è ottenuta una stima ragionevolmente accurata delle macchie focali, usando un fattore di copertura 2. I risultati numerici sono stati 1.00 mm stimato con 0.95 ± 0.20 mm e 0.400 mm stimato con 0.357 ± 0.057 mm.

L'ultimo metodo analizza anche l'effetto di un filtro fisico sulla dimensione di

macchia apparente, mostrando come essa risulti aumentata, permettendo poi di ipotizzare un effetto aggiuntivo della filtrazione alla sorgente rispetto al detector.

Nella tesi viene poi discusso l'effetto delle filtrazioni fisiche in vari setup sperimentali, in particolare facendo imaging di spessori omogenei di ferro da 1 e 1.5 cm, alluminio da 6 cm, scaletta di alluminio da 5 a 14 mm e acqua in spessori di 10 e 20 cm. Si mostra evidenza che esiste uno spessore ottimo in termini di MTF della filtrazione in funzione del materiale dell'oggetto e del suo spessore, e inoltre che la filtrazione applicata al detector ha un effetto peggiore in tutti i casi analizzati rispetto a quella applicata alla sorgente. Infatti, nei casi in cui la filtrazione peggiori la qualità immagine, la filtrazione al detector porta ad un peggioramento più evidente, ci sono casi in cui la filtrazione al detector peggiora l'immagine e quella applicata alla sorgente la migliora, casi in cui entrambe le filtrazioni migliorano, ma l'effetto della filtrazione al detector è minore e richiede spessori maggiori prima di raggiungere un valore debolmente crescente di miglioramento dell'MTF.

Viene poi approfondito, sempre sfruttando misure di MTF, quando una filtrazione in ottone sia conveniente da porre in uso e quando invece fornisca solo degradazione del contrasto rispetto all'immagine di riferimento, risultando che per elementi leggeri come l'alluminio, l'effetto è usualmente degradante perchè rimuove radiazione utile. Ci sono delle eccezioni, per le quali tuttavia il miglioramento è molto limitato e può dipendere dalle condizioni di imaging non ottimizzate per un determinato spessore, nel caso di imaging di oggetti a spessore variabile.

Viene anche posto in evidenza che l'uso di una filtrazione porta ad un miglioramento globale dei risultati di contrasto se, in un materiale con spessori multipli, viene scelto lo spessore che migliora il contrasto usando come riferimento lo spessore minore.

Alla fine vengono riassunti i risultati, fornita una panoramica dei possibili miglioramenti e continuazioni del lavoro, tra cui miglioramento della precisione di misura della posizione, aumento della statistica delle misure per ridurre le incertezze associate, utilizzo di un diverso metodo di misure dell'MTF. In conclusione vengono proposti sviluppi ulteriori, come un confronto tra griglie anti-scattering e filtrazione e il trasferimento dei risultati alla tomografia e lo studio dei risultati di diverse coppie materiale dell'oggetto e materiale della filtrazione.

Contents

Ringraziamenti	XI
1 Introduction	1
1.1 Radiography and tomography	1
1.2 Protocol creation and performance analysis	1
1.3 Structure	2
2 X-rays and radiography	3
2.1 X-rays interaction	3
2.1.1 Cross section	3
2.1.2 Radiography	4
3 Objective of the thesis	7
3.1 First intention	7
3.2 Proposed approach	8
3.3 Instrumentation	9
4 Imaging	11
4.1 Parameters definitions	11
4.1.1 Detector calibration	11
4.1.2 Tube parameters	14
4.1.3 Alignments	14
4.1.4 Console parameters	15
4.2 Uncertainties	16
4.3 Image quality quantities	17
4.4 Experimental technique	18
4.4.1 Gain, Lag and Burn in	18
4.4.2 MTF measure with IQIs	18
4.4.3 Focal spot measure with Slit Camera	19
5 Experimental results	21
5.1 Calibration	21
5.1.1 Bad pixels and dark current	21
5.1.2 Gain	21
5.2 System analysis with MTF measures	25

5.2.1	MTF(mA,kV)	25
5.2.2	MTF as a function of magnification	28
5.2.3	MTF with tube filtration	29
6	MTF measures for Focal Spot characterization	31
6.1	Classical methods	31
6.1.1	Slit camera	31
6.2	Frequency ratio	32
6.2.1	Effect of parameters on FS ratio	33
6.2.2	Use of the ratio	35
6.3	Optimal magnification method	35
6.3.1	Theoretical calculation: geometric optics	36
6.3.2	Measures of magnification	36
6.3.3	Effect of filtering on FS dimension	38
7	Application: Brass filter	41
7.1	Effect of filtration on tube and detector	41
7.1.1	Tube vs Panel filter	41
7.1.2	Experimental maximization of MTF to find highest use- ful filtration	52
7.2	Material effect	53
7.2.1	Thickness	55
7.2.2	Energy spectrum	56
7.2.3	Filtering material type	58
7.3	Non uniform materials	58
7.3.1	Imaging of 1 cm and 1.5 cm iron	58
8	Conclusions	63
8.1	Results	63
8.2	Possible improvements	63
8.3	Further developments	64
	Bibliografy	65
A	MTF value equivalence	67
B	Matlab code for automatizing of Lag computation	69

List of Figures

4.1	Schematic representation of a Flat Panel Detector exploiting indirect conversion. From <i>State of the Art of CT Detectors and Sources: A Literature Review</i> , [6], p. 77	12
5.1	Flat field exposure without gain correction, 285 kV 3 mA 0.5 s .	23
5.2	Multi-linear interpolation for power calibration	24
5.3	Example of MTF acquisition with the IQI	26
5.4	Example of measured MTF, 1.5 mA at 180 kV for medium focal spot, M=1.24, or at 20 cm from the Detector, f(10%)=2.99 . . .	27
5.5	Effect of kV increase on MTF	27
5.6	Example of measured MTF, double focal spot, effect of mA variation at 200 kV.	28
5.7	Example of measured MTF, double focal spot, effect of mA variation at 100 kV, half of above.	28
6.1	Image of a plated impressed by means of a slit camera method.	32
6.2	Trend of the Frequency ratio at MTF=10%, with M=3.088, or at 34 cm distance from the source, as function of the kV, 1 mA	34
6.3	Trend of the Frequency ratio at MTF=10%, with M=3.088, or at 34 cm distance from the source, as function of the kV, 0.5 mA	34
6.4	Trend of the Frequency ratio at MTF=10%, with M=3.088, or at 34 cm distance from the source, as function of the kV, 1.5 mA	34
6.5	Trend of the Frequency ratio at MTF=10%, with M=4.118, or at 25.5 cm distance from the source, as function of the kV, 1 mA	35
6.6	Observed behavior of MTF as a function of the distance between detector and object (IQI)	37
6.7	Observed behavior of MTF as a function of the distance between detector and object (IQI)	37
6.8	Behavior of MTF vs DDO with an applied filter of brass, thickness 0.3 mm	39
7.1	Effects of the presence of the water bottle near the IQI.	42
7.2	Effects of the presence of the water bottle placed in front of the IQI.	43
7.3	Effects of the presence of the water tank near the IQI.	43

7.4	Imaging of a water bottle in central position with 0.3 mm brass pre filtration at 180kV, 15mA at 90cm SOD, or M=1.17.	44
7.5	Post filtration of 0.3 mm brass with tank near the IQI. Parameters are 180 kV, 15 mA, 90 cm SOD, or M=1.17.	45
7.6	Pre filtration of 0.3 mm brass with tank near the IQI. Parameters are 180 kV, 15 mA, 90 cm SOD, M=1.17.	46
7.7	Effect of filtration on imaged 1cm exploiting f(0.05) variation referred to not filtered image. + sign refer to pre-filtration, the same color represent same total filtration. Imaging is performed at 350 kV and 2.5 mA, medium focal spot is necessary to produce enough power output, SOD is 99 cm, M=1.06.	47
7.8	1 cm Fe reference image, M=1.78	48
7.9	1 cm Fe with 0.8 mm pre-filtering	49
7.10	1 cm Fe with 0.5 mm pre-filtering and 0.3 post filtering	50
7.11	1 cm Fe with 0.3 mm pre-filtering and 0.5 post filtering	51
7.12	Graphical representation of MTF increase	53
7.13	Graphical representation of f increase with increased thickness and kV	53
7.14	Variation of f(5%) with filtration, imaging 6 cm alluminium at 400 kV and 2.5 mA, to be compared with 2 cm iron, same parameters	54
7.15	Variation of f(10%) of 2 cm iron imaged with 400 kV, 2.5 mA	54
7.16	Effect of filtration with different thicknesses of Al at 70 kV, increasing filtration, according to percentile variation of f(0.1).	55
7.17	Effect of filtration with different thicknesses of Al at 90 kV, increasing filtration, according to percentile variation of f(0.1)	56
7.18	5 different Al thickness, ranging from 2mm up to 1.4 cm, with 3mm steps.	57
7.19	1 and 1.5 cm iron imaged with 320kV, 3.1 mA at 100 cm distance from the tube, or M=1.05, focal spot of 1 mm, no filtration	59
7.20	1 and 1.5 cm iron imaged with 320kV, 3.1 mA at 100 cm distance from the tube, M=1.05, focal spot of 1 mm, with 0.5 mm filtration	60
7.21	Ratio between 1 and 1.5 cm regions, difference between 1 and 1.5 cm regions, and percentile increase of f(0.05) passing form 1.5 cm region to 1 cm region, without and with filtration respectively	61
A.1	Behavior of spatial frequencies for given MTF values at different mA, fixed kV	67

List of Tables

5.1	Grey values obtained as function of mA and power. Errors are calculated by difference between linear interpolation of the selected point, obtained with the nearest points, and the measured value. Grey values range runs from 0 to 65535.	23
5.2	Gray values as function of kV and power.	24
6.1	Comparison between Focal Spot (FS) dimension, optimal magnification and Detector Object Distance (DOD) in this system .	36
6.2	Comparison between observed and theoretical calculations of the focal spot dimension for the two tubes	38
6.3	Comparison between Focal Spot dimension with and without pre-filtering	39
7.1	1 cm Fe MTF increase from reference with increasing tube filtration	52
7.2	1.5 cm Fe f increase from reference with increasing tube filtration	53

Ringraziamenti

Ringrazio tutte le persone che mi hanno supportato durante il mio percorso di studi magistrali.

Ringrazio il mio Relatore e Professore Marco Caresana, per la sua disponibilità, gentilezza e preparazione professionale.

Ringrazio il mio Correlatore, Ingegnere Davide Baratto, per la sua disponibilità e l'aver condiviso con me parte della sua esperienza professionale, ed insieme ringrazio la Gilardoni S.P.A. per aver collaborato e contribuito allo svolgimento di questa tesi.

Ringrazio la mia famiglia, in particolare mia madre Paola, per il supporto che mi hanno fornito, in particolare in questo difficile periodo dovuto alla pandemia mondiale.

Ringrazio la mia fidanzata Giulia, per il suo supporto costante ed infaticabile, la sua dolcezza e solarità, la sua pazienza e il suo umorismo, che mi hanno permesso di rimanere resiliente dinnanzi a tutte le avversità di questo viaggio. Mi sei sempre stata accanto e mi hai aiutato tanto, grazie davvero.

Ringrazio tutti i miei amici ed amiche, ma vorrei fare qualche ringraziamento in particolare. Grazie a Gianfranco, il mio amico di più lunga data, sempre presente, con cui condivido i ricordi di Praga e tanti altri. Grazie ad Ennio ed Edo, grazie veramente, per tutte le risate e per tutti i momenti più assurdi, non mi sarei annoiato neanche volendo con voi. Grazie a Jack, insieme dal primo anno, e al nostro stupendo viaggio a Berlino. Grazie a Pier, che mi ha sempre teso una mano e regalato una risata e consigliato in ogni momento, con la sincerità che lo contraddistingue e il spirito incredibile. Grazie a Julian, che mi ha fatto superare la prima sessione magistrale, mostrandomi che si può essere matti ma anche geniali. Grazie ad Haffsa, ad Antonella e a Silvia che mi hanno accompagnato durante questi due anni speciali condividendo esami, progetti e aperitivi. Grazie, a tutti i ragazzi del Collegio, dai più vecchi alle matricole, e a tutti i Salesiani.

Da ultimi ma tutto fuorchè ultimi, un grazie speciale a Marco e Riccardo, due persone stupende con cui ho condiviso tutti i miei anni di università, mi avete insegnato molto e fatto crescere tanto, avete reso veramente significativi questi anni e i momenti insieme a voi sono i miei ricordi più belli.

Grazie a tutti voi, che con me avete condiviso tante cose, ma soprattutto voi stessi. Grazie di tutto.

Chapter 1

Introduction

This thesis work was performed in collaboration with Gilardoni S.P.A.

1.1 Radiography and tomography

Radiography and tomography are two techniques widely spread to investigate and represent matter. The main aim of this thesis work is to analyze some properties of systems exploited in such techniques in the industrial manufacturing field.

1.2 Protocol creation and performance analysis

The problem we are facing is the lack of documentation providing the detailed procedures to evaluate performance of industrial radiographic and tomographic systems. We can find some references that ascribe how the performance must be tested, namely the ASTMs, like *Standard Practice for Digital Detector Array Performance Evaluation and Long-Term Stability* [1], but many aspects are left to manufacturer and user's agreement. This work has the purpose to identify some parameters to evaluate the imaging performance, for specific industrial applications, of radiographic and tomographic systems or some components of the systems. The first steps come from well known books, such as *The Essential Physics of Medical Imaging* [2], *Handbook of X-ray Imaging. Physics and Technology* [3], *MEDICAL IMAGING. Principles, Detectors, and Electronics* [4] or *Industrial X-Ray Computed Tomography* [5], that allow us to define meaningful quantities to analyze and to understand the structure of the system and their components. From this starting point, we chose the indicator that is both meaningful and practical, the Modulation Transfer Function, or MTF in short. We would like to use the DQE, Detective Quantum Efficiency, a quantity that derives from the MTF but includes explicitly the contribution of the noise to the image by means of the Noise Power Spectrum, for radiography, but the additional effort required was way beyond the aim of this work. This is

due to the nature of the DQE, that requires to evaluate the exposure in terms of photon fluence for a give quality of the x ray beam, so this characterization would have been impractical and the noise contribution don't seem to be so enhanced.

What comes next is the evaluation of the specific parameters modifying them and the system response and its uncertainty, with some solutions that can improve the system's overall performance, such as filtering, and their limitations. The works end with some considerations on possible works starting from this one.

1.3 Structure

The structure is the following:

In the second section we cover the introduction to X-rays physics and its application to radiography;

In the third one we are going to describe the object of this thesis work, how it started and its evolution;

In the fourth section we describe the quantities of our choice to characterize the systems in study, their definitions and their meanings;

In the fifth one, it is presented the experimental results for preliminary system analysis and evaluation of MTF measures with different parameters in this system;

In the sixth one, it is described a classical method for focal spot measure, and then two innovative method are proposed and analyzed;

In the seventh section it is presented the application of one method to physical filtering performance evaluation according to MTF measures;

In the last chapter, it is discussed how this work can be used as starting point for further analysis and its possible improvements.

Appendix A shows the equivalence in the choise of MTF representative value for 0.5, 0.2, 0.1 and 0.05.

Appendix B reports the code used to automatize the computation of the Lag.

Chapter 2

X-rays and radiography

This section is devoted to a brief recall of X-rays physics and introduction of digital radiography imaging. The reader possessing a prior knowledge of these topics can move on to the following section.

2.1 X-rays interaction

The X-rays radiation, due to its typical energies, is mainly described through intensity in terms of photons number and direction in terms of straight line propagation. In other fields of optics we can face exponential description with amplitude and phase. This approach is followed when talking about phase contrast, since this innovative techniques exploits the undulatory behavior of X rays instead of its photon-corpuscular behavior.

2.1.1 Cross section

To describe the probability of photon interaction with matter is then convenient to introduce the cross section, that has the dimensions of an area, but it has some special meaning. The meaning of this quantity can be explained in probabilistic terms, saying that if the photon hits the cross section area, then it interacts, otherwise it passes through without interacting. Notice that the cross section area is not coincident with the atomic or nuclear dimensions, since it depends on the processes considered. It can be defined for a single process or for the total probability of interaction. For X-rays we can consider 3 processes characterizing our discussion:

- Compton scattering;
- Photoelectric absorption;
- Pair production.

The set-up used for the development of the thesis work has a maximum nominal energy of 450 kV, which means that we can neglect the contribution of pair production to the total cross section. This also implies that the observed

phenomenology will depend on either Compton scattering or photoelectric absorption.

One concept, different viewpoints

Since the cross section describes the interaction of two particles, in our case a boson and a fermion, we can distinguish 2 different families of cross sections, depending on the viewpoint:

- Total and photo-electric cross sections;
- Total and absorption;

Since we neglected, due to our energies of concern, the pair production phenomenon, we can say that the Total cross section is the sum of photo-electric and Compton cross sections. It is distinguished between absorption and photo-electric, and it is just a matter of viewpoint as already said. Absorption means that the photons are removed from a trajectory that is able to reach a useful area of the detector. The total cross section is always the same, what changes is its use. Thus, the difference between the total and the absorption cross section represent the scattered radiation that is deviated with an angle sufficiently high that either it does not reach the detector at all, or it reaches the detector producing noise. I'd like to highlight that *not all of the scattered radiation becomes noise*. This is one of the main difficulties introduced in Monte Carlo codes of these problems, since they become very object-specific due to the strong geometric dependence and, furthermore, the great variety of object types, materials, dimensions and geometries.

In the following, we are going to use a phenomenological approach, so we won't perform MC calculations, but I think that this kind of reasoning will simplify the following discussion's understanding, since we will look at noise, uncertainties and precision, but also at contrast, resolution and filtering.

2.1.2 Radiography

Radiography exploits the properties of absorption of materials in order to determine their thickness or their density. Let's have a closer look to it. Let us consider, exploiting the Lambert-Beer law, an exponential absorption of photons when interacting with matter.

Unique material case

In a uniform material composed by one atomic species we would observe the following behavior for a monochromatic beam, without considering subsequent emissions of X rays by the material irradiated:

$$I = I_0 * \exp(-(\mu/\rho) * x * \rho)$$

We can see that there is a dependence on the initial photon number I_0 and an exponential dependence on the thickness of the material, x , and on the density of the material. Strictly speaking, x is not the material thickness, but the path length that a photon travels. This writing is used, because the mass attenuation coefficient μ/ρ is a constant depending only on the atomic nature of the material, so it can be calculated and identify the material causing the attenuation. Let us say that air is transparent for X-rays, so we will consider air as vacuum. however, in industrial applications is not uncommon to face different materials and/or different material thicknesses, as in the case of filtering, see 7.

Multi-material case

Considering again a monochromatic beam, but subsequent different types of materials, due to exponential dependence, attenuation does not consider the order in which the radiation meets them, so we can make a summation of the exponents:

$$I = I_0 * \exp\left(-\sum_i (\mu/\rho)_i * x_i * \rho_i\right) \quad (2.1)$$

This equation considers x_i as the path length travelled by the photons in the i -th material. This is a fundamental point, since attenuation depends exponentially on this length, so every added material will produce a strong attenuation but if it has a low linear mass attenuation coefficient and x is limited inside it.

The above discussion can be extended to a non-monochromatic spectrum by considering a different attenuation for each energy.

Radiography set-up

In order to perform a radiography we need something that is able to reveal the radiation and to collect it, that in our case is a Flat Panel Detector (FPD), so we are talking about **digital radiography**(DR), coupled to the electronics used to acquire the signal and display it on screen, and an object to be analysed. We will recall the main concepts useful for our discussion, the reader can find more in textbooks such as [4] and in the review *State of the Art of CT Detectors and Sources: A Literature Review* [6].

The X-rays tube exploits a metal wire, called Cathode, through which current flows in the order of mA. This will be one of our controlled parameters. The electrons are extracted from the wire by means of a potential difference that has the order of the kV, and this will be another parameter. The electrons extracted from the wire are driven to a tungsten target that is the Anode. The anode is set inclined with respect to the electron flight direction and their interaction with the target produces Bremsstrahlung radiation. Please note that tungsten is exploited both for its high Z value, producing non negligible bremsstrahlung, and for its high melting point. The power supplied to the

anode target is one of the limiting conditions of the set-up. X-rays emerging from the anode are collimated by means of lead collimators, since lead is the highest Z material that has stable isotopes. The inclination of the anode provides different projections of the impinging electrons area to the collimators side, giving the focal spot dimension. Focal spot dimension, along with pixel size, are the critical geometric factors for the image quality of the set-up. Lower dimensions of focal spot and pixel size lowers the minimum spatial resolution, but they have some drawbacks. It will become soon clear that *trade-off* is the key concept of our discussion.

Chapter 3

Objective of the thesis

The aim of this work was looking for improvements easily adoptable in the system under study and to produce a practical procedure to address the performance of the system, in such a way that both customer and the Company are satisfied and technicians do not spend a lot of time in tests, or they need to bring with them a large number of test objects, even for routine analysis.

3.1 First intention

At first, what the Company proposed was the creation of an internal protocol of testing for the imaging systems. Then, studying literature concerning mainly tomography, two factors were considered. The first one was that a new whole standard was under elaboration by the ISO, so that a completely referred procedure should probably be changed in a year or two; the second one was that, depending of the grade of deepening required by the accreditation, the work could increase extremely in complexity and work volume. In fact, at the present moment metrology with these kinds of techniques has an important issue regarding the quantification of uncertainties. There are a large number of recent studies on this subject, as for example *Estimation of measurement uncertainties in X-ray computed tomography metrology using the substitution method* [8] is a useful guideline with clear identification of the state-of-the-art equipment, and the mechanical positioning system needed has to be really precise, the electronics is checked to estimate the uncertainty it provides, as also is done with temperature in the cabinet and in the tube and detector. Since this topic is so extended and the instrumentation at hand is adequate, even if not at the level described in the above-mentioned paper, a different route for the present work was chosen.

3.2 Proposed approach

Even if this work is not thought as a reference, it can be taken anyway as a starting point to implement an effective and innovative method to speed up the production of an internal procedure, using just a small Image Quality indicator, IQI, and some data analysis that can be also automatized if these methods are applied to standardized situations. The use of the IQI is described in the ASTM standards, and we used the [1], *Standard Practice for Qualification of Radioscopic Systems* [10], *Standard Practice for Determining Contrast Sensitivity in Radiology* [11] and *Standard Practice for Determining Total Image Unsharpness in Radiology* [12].

The IQI, or Image Quality Indicator, is an object standardized that is used to measure some specific quantity related to image quality. In the case of the one used here, it is made by a series of wire pairs made of lead, that have a specific diameter and they are placed at a distance equal to the diameter. There are several pairs in a single IQI, they are placed from the wider to the closer pair.

Difficulties

The main problem in creating a rock-solid procedure is that quantification of uncertainties is incredibly laborious and in the best case what can be done at the moment is exploiting uncertainty budgeting seen in [8], in tomography the problems multiplies due to reconstruction algorithms, longer imaging times, surface determination and many other characteristics. Since the system is not adequate to perform precise dimensional measurements, what was decided was to let this topic outside of the discussion, introducing adequate esteem based on observations and error propagation formula. Since there is no feedback for some quantities, such as mA and kV actually provided by the power electronics, the first figure of merit has to be adequately evaluated, and since it shows some dependence on them, stationary points are required to be selected in the function, in order to minimize the error. Since the values of kV and mA specific for the measurement do not influence the outcome, it is important that the kV and mA provided to the system are always the same, even if different from the input request.

Chosen method and applications

The second one, instead, showed some robustness with respect to parameters changes, and it was exploited since it provides a value independent from a reference, allowing interesting considerations, in particular in the present case, where a precise measure with classical methods was not performed. Its main drawback is that it is a little more laborious to perform, however it is neither

complicated once explained, nor susceptible of strong errors or difficult interpretation of results.

It could suffer from some type of bias; however it was not possible to prove it in absence of precise measure instrumentation. Anyway, obtained results do not depend on the specific values obtained but on their relative values, exception made for the comparison between obtained and nominal results.

3.3 Instrumentation

The instruments used to perform these analyses:

- Cabina XE-L HE, by Gilardoni S.P.A.;
- IQI EN 462-5;
- Brass filters;
- Iron and aluminium thicknesses, water containers;
- Polystyrene support.

Example of obtained imaging is shown in 5.3; there, it is clearly visible the shape of the IQI.

The cabinet has 450 KV as maximum tension output and a total power of 1200W. The detector is a solid-state detector, in particular a flat panel detector with pixel size 200 micron.

Supplementary specification can be found in the technical data sheet of the machine.

Brass filters are not thicker the 1 mm, but they can be superimposed to create thicker filters.

Chapter 4

Imaging

The quantities relevant to our discussion depends mainly on:

- power of the signal;
- noise;
- spatial resolution;
- uncertainty.

There are many quantities that required to be evaluated in order to produce a complete characterization of the imaging system, but as said the aim of this work is specific, so they will not be addressed all. We will focus on contrast, but we need to understand the main components of the system and their functioning principles, so that effects can be understood.

4.1 Parameters definitions

To simplify the structure of the discussion, we will subdivide it according to main components and analyse what aspects have to be observed carefully.

4.1.1 Detector calibration

We have to calibrate the Flat Panel Detector, or FPD. It is a solid-state detector made of amorphous a scintillator, and a photodiode with a silicon Thin-Film Transistor arrays, a-Si TFT, constituting the pixel. As scintillator it is exploited caesium iodine doped with thallium, named CsI:Tl. Its working principle, schematized in figure 4.1, is that incoming X rays interact inside the scintillator, then conversion of radiation re-emitted by the scintillator into charge pairs inside the photodiode. It is said indirect conversion opposed to direct conversion, which exploits amorphous selenium without a scintillator component.

Before starting the measures, we have to check for:

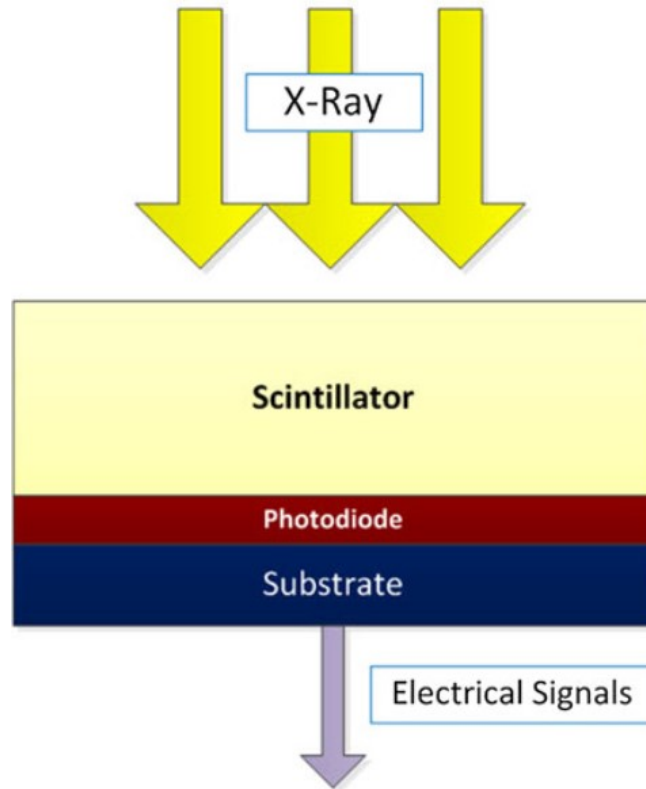


Figure 4.1: Schematic representation of a Flat Panel Detector exploiting indirect conversion. From State of the Art of CT Detectors and Sources: A Literature Review, [6], p. 77

Bad pixels

Talking about bad pixels, we refer to those pixels that are damaged or simply do not operate with proper effect. the ASTM [1] provides definitions for them and how to compensate, operating opportune averages between working pixels and assigning that values to damaged ones.

Since the Company was following the exact procedure indicated inside the ASTM, correction was already performed.

Offset

Offset is the term due to background that shows up with X-rays off. The offset is produced by what is called Dark Current, that is the signal provided to the detector when the X-ray are off, so when it is "dark". This noise consists of charges created inside the detector, even if there are no incoming photons, mainly due to thermal motion of charge carriers.

Once again, the Company was following the procedure indicated in the ASTM, so there was no need to study this subject, since the temperature inside the cabinet is not controlled. More on dark current can be read in *Springer Handbook of Electronic and Photonic Materials* [13].

Gain

Gain is the variable term that changes with energy or power, that corrects for pixels response to radiation, in order to provide a uniform image in absence of an object. It is calculated using the so called flat field exposure.

Gain was tuned by the Company acquiring 4 values at 15%, 35%, 50% and 65%, creating a multi-linear interpolation.

Since it was quite common to reach powers in the order of 80% of the range of the detector, I evaluated the error due to estimate the 80% power with fixed mA or kV. Since introducing one more point is quite fast and does not require specific formation to be performed, it was found that taking one more point could reduce the error by 5% in the worst case analysed, in most cases it is around 2%. Since the procedure, as already mentioned, is quite fast and easy and it has to be performed anyway, it is worth doing it.

Lag

The lag is the time that is needed by the detector to return to its initial value following an acquisition. Here, even if the Company was following the ASTM procedure, they did it manually, while it is possible to write a code to automatize the procedure once the images are acquired. The code is written in Matlab and is reported in B.

Burn in

Burn in is the effect on the image that is realized just after that a long and powerful acquisition has been completed. It is an important parameter in radiography, in order to understand what an adequate time is to wait before proceeding with another imagine. It is even more important in tomography, where many frames has to be acquired and the time of imaging can be quite long, inducing this kind of effect and let it increases in its severity. Optimization of this parameter was not performed, since there was no need to perform large sequences of acquisitions.

What was discussed was the idea to compensate for it tomography, creating a precise characterization of the time in which this phenomenon occurs in the set up. Then, if during a tomography, a frame is taken before going forward with the object rotation, propagating in time the expected grey values, it is possible to "clear" the following image. It is of great advantage if the imaging time is large and is affected by strong ghosting effect, that is the previously acquired image showed as a vanishing "ghost" superimposed to the following one.

Linear response

The linearity response of the detector is a feature required to link what reaches the detector and what the detector collects and can be converted into image.

Usually, when it is addressed this topic, we are mostly concerned about **energy** linearity, mainly because we are interested in spectroscopy. Here, instead, what is of our concern is the photon fluence along with energy, because the interaction with the materials is a function of the energy. In order to take into account both, what was addressed was the *linearity with respect to power*, calculated as the product between mA of current in the tube cathode and kV for electrons acceleration, that is what characterizes the spectrum in a fixed set up. The linearity will be addressed further in 5 during the calibration procedure.

How the parameters not discussed are measured can be seen in the ASTMs.

4.1.2 Tube parameters

Concerning the tube, we have to look at:

- Focal spot dimensions;
The focal spot characterization will be one of the main objectives of the thesis, thus we postpone the discussion to the chapter 5 and following ones.
- Uniformity;
The uniformity of photon fluence upon the detector is usually a not acceptable hypothesis, so we have to check if it is correct and understanding its validity range when using it. This can impact the measures and the imaging production itself.
- Temporal stability;
Stability in terms of time can have 2 meanings. First, let's consider a fast acquisition, we have to perform at least a small integration between images acquired in order to compensate for fluctuations in the number of photons coming on the detector. Temporal variations are due to the typical statistical Poisson's behaviour of photons, but it can also be enhanced by the inability of the tube system to provide stable kV and mA through the time of acquisition. Then, a second meaning refers to stability of the parameters of the tube considering scanning time that is large. Since we have an heat build-up of the anode, its performance can vary over time, and it is of concern if different acquisitions keeping X-ray on for long time are compared, but it is of even greater concern in tomography, where typical scanning time can be of tens of minutes up to hours.

4.1.3 Alignments

After tube parameters, in a practical perspective, we have to consider alignment parameters, that can introduce errors mainly in tomography, but in radiography can affect repeatability of the measures. The main source of error due to alignment are:

- Source-Detector (SD) alignment.
It is performed using projection phantoms produced by the Company itself.
- Supporting plate tilt along SD direction.
If this error is present, it can introduce more critical problems depending of what we are looking for. If we are studying spherically symmetric objects or voids, this is not something so impacting, while considering metrology it is a mainly cause of errors, since geometrical projections get distorted and the only conserved is the spherical shape.
- Supporting plate tilt in plane perpendicular to SD direction can be compensated thanks to software correction.
This parameters address *static alignment*. We could say that that's enough, since the system is usually still while performing a radiography. Nonetheless, we must move the system before acquiring an image, in order to tune the magnification, the position on the screen and we may want to rotate the object, so we can describe these points using *dynamic* parameters. Let's consider the movement the system can perform, posing as reference system the detector surface, calling z the direction from the detector to the source and placing X-Y plane on the detector surface. We have the following degrees of freedom:
 - Supporting plate rotation;
Rotation is of primary importance in tomography, while in radiography it is just a matter of fast arrangement of the desired object orientation since homogeneous steps are not required to be performed.
 - Supporting plate translation along z and x directions;
 - Source and detector vertical translation;
 - Coordinated tilt of source and detector, using the plate center as rotation center.

4.1.4 Console parameters

The console parameters are the physical quantities that can be used to tune interaction with the object through the imaging system.

- kV
The kV are the unite of measure of the potential difference used in order to accelerate the electrons inside the X ray tube. The characterized the maximum energy of the spectrum and, once filtration effects are evaluated, it addresses the whole distribution of energies. It is an important parameter, since it is the first to be tuned when imaging, because the energy has to be enough to pass the material and let the photons reach the detector, but not so high to reduce the interaction of the photons with the medium to be inspected.

- mA
The parameter of mA is used to improve image quality. The mA do not change the relative contribution of scattering and photoelectric absorption, but change their absolute value. As such, the image can increase its brilliance and contrast and the noise is reduced in its relative contribution. However, pay attention that mA ranges from 0.5 to 9 in this kind of systems, so it could be easy to reach saturation of many pixels if it is not taken into account that power increases sharply with mA at high kV.
- Exposure
Exposure is an important parameter that need accurate evaluation for its use. Its main pros are the reduction of noise and an increase in brilliance since more charge is collected inside the detector electronics per image. Its main drawback is that imaging time increases. This can be of small concern in radiography, but it is of extreme importance in tomography, where a series of radiography images can count up to 2000 acquisitions. During all of this work acquisitions, exposure is fixed at 0.5 s.
- Integration
The system under study has as default setting a minimum integration of frames, that is the one used during all the imaging tests. Its main advantage is the reduction of randomly distributed noise, but, as exposure does, it increases the imaging time.

4.2 Uncertainties

Uncertainties are an hot topic in radiography and tomography. An extended review referring to both radiography and tomography is *Review of the influence of noise in X-ray computed tomography measurement uncertainty* [14]. We will address uncertainty mainly in two ways:

- A type-A uncertainty associated to photon physics and material physics;
- A type-B uncertainty, evaluated by myself based on the experience acquired performing these measurements and personal evaluations. This contribution can be quite large and usually is the prevalent one, since it tries also to consider many error sources, as systematic errors, positioning errors, kV and mA output uncertainty not quantified here, and non-homogeneity of materials under inspection. These types of errors are applied to meaningful measures and then, provided a mathematical correlation with quantities of interest, error propagation is used to provide the final errors.

4.3 Image quality quantities

The quantities that is suggest to have quite confidence with are the following ones, more about them can be found in [2] or in [7] : The **Signal to Noise Ratio** is defined as:

$$SNR = S/N \quad (4.1)$$

Where S is the signal intensity and N is the noise of the image. The **Contrast to Noise Ratio**

$$CNR = \frac{S - B}{B * N} \quad (4.2)$$

Where B is the background.

The **Modulation Transfer Function** is defined as the effect in terms of SNR on the image, provided by the imaging system; it is the ratio between the SNR output to the SNR of input.

$$MTF = \frac{SNR_{out}}{SNR_{in}} \quad (4.3)$$

The MTF is higher as the degradation provided by the imaging system is lower. It depends on the distance and dimensions of two objects, but it is usually expressed as a function of the spatial frequency. Spatial frequencies are linked to object dimensions and are measure in line pair per millimetre, lp/mm. The dimension of the object is converted in lp/mm calculating how main wire pairs of diameter equal to the object, placed at a distance equal to their diameter, can be placed inside a millimetre.

The MTF is often used as the main indicator of the system performance when DQE is not used. In the industrial framework, it is common to refer to the maximum spatial resolution, that is the minimum distance between two objects that the system can resolve. This can be little tricky, since we have to define what does "resolve" mean. There are several conventions, we will use the most suited from case to case and in appendix A we discuss the validity of our approaches and limitations to these considerations. Where not specified, we are going to use the convention that a value of spatial frequency providing a value of MTF of 0.1 is the reference of resolution. This choice come from the aim of this work. The value of 10% is the most suited one, since it takes into account every aspect of the system, but it is particularly sensitive to small changes in the optical system we are interested in. It is also quite stable with respect to fluctuations due to photons statistics, since at 10% we usually have enough photons to keep type-A error under control. The only case in which the value will be used of 5% is a case in which the spatial frequencies of the IQI are pretty much high for the thicknesses under analysis, so that 10% was no longer a representative value of the MTF curves. What has to be considered when selecting a value of MTF as reference is that it has to be stable with respect to errors, but also sensitive to changes of interest and influenced by the interested region of the curve, not just a portion. Regions of the curve are differently

affected by the system and have different effects on image formation. The MTF, from the detector point of view, can be described as the Fourier transform of the response of the detector to a line source of radiation. The response is called Line Spread Function, and can be obtained using a slit, like in slit camera method, or by integration of the response to a point source, but it is quite difficult to produce a real point source, or using the derivative of an edge. More on these topic can be found in several books, as in *Introduction to biomedical imaging* [9].

4.4 Experimental technique

We have defined the quantities. Now, we have to explain how we are going to measure them on field. The ASTM [1] describes it, so we are going to recall briefly them here.

4.4.1 Gain, Lag and Burn in

- Gain
Gain is measured using a series of images with bad pixels and dark current corrections, taking the mean values of a specific area, and then correlate power with the obtained grey values.
- Lag
Lag is measured using 4 images without gain and offset corrections, the first is the reference with x rays off, the second is the reference with x rays on, the other row are two subsequent inside the series of acquisitions made while x rays are switching off, because the measure is devoted to address the dynamic of shutdown of the detector, so X ray must not be already off. It is defined as the percentile ratio of the mean gray values in a specified ROI, of the difference between the grey values of the selected image and the "X ray on" image, both subtracted by the dark image.
- Burn in
Burn in has its specific procedure, it was not performed. It requires to evaluate the difference between two areas of the detector, one exposed to radiation directly, the other one with a reference object for specific times.

4.4.2 MTF measure with IQIs

MTF is measured by means of wire pairs. The evaluation is performed by means of a tool in the user interface of the program Delfis, which allows to draw and area or line and observe the gray values along them.

Delfis is a software that shows real time image of the object, but can be used also in a static modality, stopping the acquisition of the incoming signal. It allows to modify the image using contrast and brilliance, image filters and

other features. Here, it was exploited to collect the images and to read the grey values displayed inside an operator-specified region. From the grey values graphic, it can be read the minimum value, corresponding to one of the two wires, the central maximum, corresponding to the space between the wires, which has the same width as the wires diameter, and the background value, taken outside the pair. the MTF is ≤ 1 . Then, we can calculate:

$$MTF(f_x) = \frac{Max_{f_x} - Min_{f_x}}{Background_{f_x}} \quad (4.4)$$

Where f_x is a given spatial frequency indicated by the Image Quality Indicator.

The link between 4.3 and 4.4 is that the term SNR_{in} is assumed to be equal to 1, while the term SNR_{out} is calculated as the signal, represented by $Max_{f_x} - Min_{f_x}$ at a given spatial frequency x , divided by the noise provided by the background, that is the value of background near the maximum at the same spatial frequency x , $Background_{f_x}$.

In many cases, since the measures are not so precise performed this way, approximating the background at a given spatial frequency with one representing the background around the IQI do not introduce appreciable errors, since we are not interested in values under the point percentile.

The MTF is the calculated by means of an interpolation of the points obtained at different spatial frequencies, with a polynomial fourth-grade function, fixed that $MTF(0)=1$. There are few cases in which this condition is not met by the interpolation, but it is due to the strong absorption of the medium. This can be adapted using a different IQI, with lower spatial frequencies. When this happens, if the IQI cannot be changed, it is also wise to let this requirement out of the interpolation.

4.4.3 Focal spot measure with Slit Camera

The measurements with the slit camera were performed twice per focal spot. It was measured using a slit in a metal plate and a support for a teeth plate. The plate is imaged and then developed, to obtain a shadow, that is a magnification of the focal spot. However, when they were performed, the maximum resolution of the graduated lens was 0.5 mm, so it was not able to perform a precise measurement, but it gave an order of magnitude for the focal spots. The resulting shadow is measured. In 6.1 it is shown the results of an acquisition and it is commented in chapter 6.

Chapter 5

Experimental results

We are going to analyse in detail what kind of test we performed in order to understand a specific problem and will present adopted or possible solutions.

5.1 Calibration

Calibration was the starting point for our work. The Company asked for a check-up of their procedure, in order to gain confidence with the instrumentation and with the possibility to find out possible improvement.

5.1.1 Bad pixels and dark current

The calibration in terms of bad pixels and dark current is regulated in detail by the ASTM [1] so it is not possible to provide any different solutions. We recall that bad pixels are defined as pixel that do not work correctly. They can be broken, then they do not respond to incident radiation, or partially working, then their response is not adequate to the stimulus, according to their fabrication standard. They are compensated by operating a mean with the adjacent pixels that are working. The pixels are told to produce a map, and bad pixels can be manually selected on that map.

Dark current is the current seen by the detector when X-rays are off and the panel was not exposed for an adequate time interval, so that lag and burn in do not contribute to this phenomenon. The dark current is present due to the temperature and defects of the acquisition system and consists in current produced when there is no incident radiation. We can compensate for the mean value of the dark current, acquiring an adequate image.

5.1.2 Gain

What comes next is to consider the gain. The adopted method was and is a change in gain with the tube power output. The selected values for a switch from one gain value to the other were 15% power output, 35%, 50% and 65%

and it was proposed to add one or to move them from their present percentile value.

Why power?

Let's comment first why calibration with power.

When we work in a Lab, what is of interest in a spectrum acquisition is the identification of the incoming energies, and they are displayed as counts. But what the Flat Panel Detector does is not a spectrum acquisition, it is an acquisition of incident radiation by direct or indirect conversion, which produces an output that depends both on energy and incident photons number. Then, what has been chosen is to choose the gain according to the expected incoming power calculated as:

$$P = mA * kV$$

This provides a good estimation of the charges produced, since a more energetic photon will produce more excitation in the scintillator element and more photons will also increase the number of ion-electron pair produced.

Threshold of change

The response of the detector, in terms of power, is not granted to be linear. Usually, it has good linearity properties with energy within specific ranges, but we are going to switch gain also at constant photon energy. To preserve linearity, what we can do is to subdivide the power range in regions, and to apply to each region a specific calibrated gain. The Company was used to adopt the above thresholds of 15%, 35%, 50% and 65%, but this choice leads to accept errors at high powers, since it lets a non-negligible range of energies and mA without proper calibration. So, it was proposed to select also another threshold, 80% of maximum power. This value was selected to maintain a step that was a good compromise between processing time reliability of the imaging information, keeping the power in linearity zone.

In case of thick objects, a power output approaching the maximum is needed, however the heavy beam attenuation keeps the detector output far from saturation.

Working at 80% full power (FP), the error using linear approximation is reduced. This evaluation was done acquiring points at the selected % and estimate the obtained value using the data from the two closer points. For instance, 80% FP was estimated using 50% FP and 65% FP. Similarly, 65% FP was estimated using 50% FP and 80% FP. The value of mA was taken constant for each calibration, except in one case showing the reason why moving mA at constant KV is not an appropriate solution. 3 series of data sets were acquired. A graphical example is reported in 5.2 for 2 mA calibration.



Figure 5.1: Flat field exposure without gain correction, 285 kV 3 mA 0.5 s

mA	15%	35%	50%	65%	80%	err.w.65%	err.w.80%
2	10749	24140,7	34149,9	44343,3	54922,6	-1,521%	0,431%
2.2	10324,1	24145,4	34630,7	44806	58393,6	-5,844%	3,808%
3	10618,8	23834,6	34388,1	44132,3	55177,6	-0,849%	1,474%

Table 5.1: Grey values obtained as function of mA and power. Errors are calculated by difference between linear interpolation of the selected point, obtained with the nearest points, and the measured value. Grey values range runs from 0 to 65535.

A systematic underestimate result is observed for the set of data excluding the 80% point, as reported in table 5.1. Including 80% point and we exclude the 65% one, a better estimation is provided by a linear interpolation.

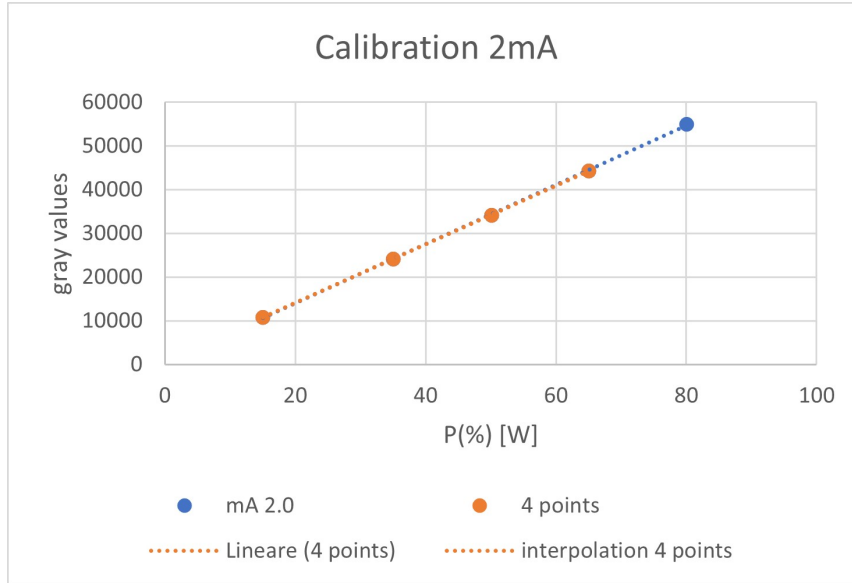


Figure 5.2: Multi-linear interpolation for power calibration

It is worth to observe that the displayed grey values are not constant, even if in some cases can be justified by uncertainties, we can say that the responses vary weakly with energies, and these increases are not monotone. Keeping the kV constant, the calibration is a little more difficult since it is harder to proceed in adequate steps. Nonetheless, a test with 2 values was performed, showing however that the overall calibration is harder due to the choice of the values with large steps and the calibration exclude one of the main variables, the energy.

Values are reported in the table 5.1.2. Errors provided by the two series of measures are quite hard to be compared, due to differences in power percentile values.

300 kV	P[%]	400 kV	P[%]
9745	14	12796	18
23277	34	35526	33
34950	51	35526	52
44634	65	45667	67
54259	79	55711	81

Table 5.2: Gray values as function of kV and power.

Looking at figure 5.1, two important features are shown. The first one regards the distribution of photons arriving on the screen, that is due to a small rotation of the x ray tube. This effect is not linked to the position of the focal spot, it is due to the production of X ray via bremsstrahlung, so the heel effect more

evident the more the anode surface is perpendicular to the electrons beam. The heel effect is observed in systems exploiting bremsstrahlung radiation, it consists in a reduced X rays intensity as the emission direction is closer to the target surface. This is due to the fact that produced X rays travel must a longer distance inside the high Z anode material and they are strongly absorbed inside it.

The second one is that the response of the pixels is divided in columns, highlighting the fact that, pixels are disposed as a grid. This is a fact that has to be considered carefully when studying anti-scattering grids applications.

5.2 System analysis with MTF measures

We already discussed about the MTF briefly, but we didn't say how powerful can be this quantity a quality indicator to perform analysis. We can use it to obtain information about detector performance, but also to collect useful information about tube performance and consumption, as performed in *Computed tomography x-ray tube life analysis: a multiyear study* [16], filters usefulness and many others. In medicine, it is preferred to adopt the DQE, in order to compare different technological solutions, but the MTF is more than appropriate considering the same system and its different features and its easiness to be measured.

5.2.1 MTF(mA,kV)

It is well known that the MTF has a strong dependence on mA and kV, as analysed in [15], so the first analysis performed on the system was devoted to the understanding of this dependence. Exposure was always maintained constant at the value of 0.5 ms.

Effect of kV increasing

It is quite evident that increasing the kV applied decreases the values of MTF as a whole. In particular, we are going to address the changes in the MTF looking at the spatial frequency, measured in line pair per millimetre (lp/mm), at which the MTF reaches the values of 10%. We can see that in 5.5 the MTF yellow function comes from 200 kV and 1 mA. Increasing the kV from 200 to 250, the MTF lower down to the blue line, that lies entirely under the 200 kV MTF function. This result is expected, since higher energies are less attenuated from the IQI material due to a lower photoelectric cross section, thus the contrast is reduced. The effect suggests to use the minimum energy required to form the image, also said the one required *to pass the object*. Please keep in mind that this statement is true if we can neglect beam hardening artifacts formation, and it is not always possible.

Those graphics are generated using the smaller focal spot. Notice that the

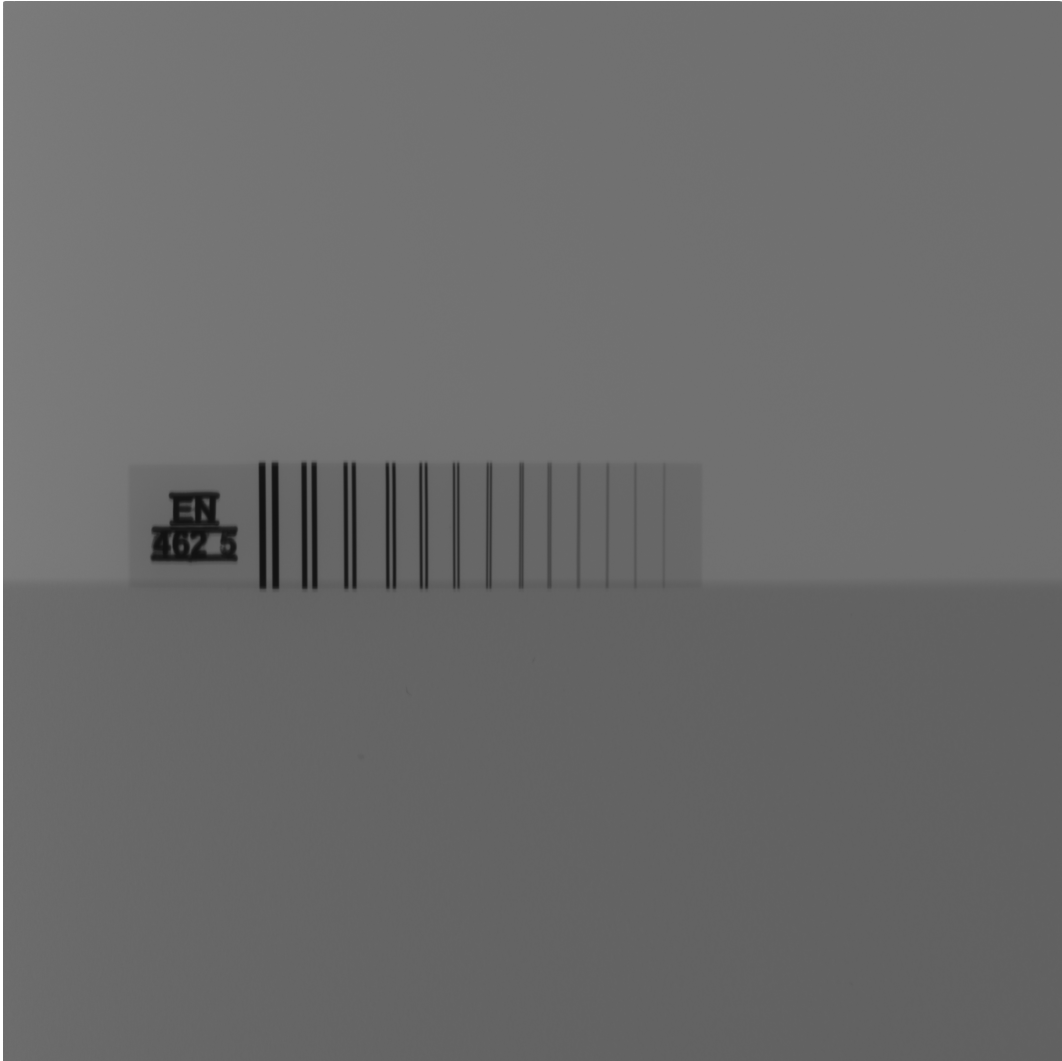


Figure 5.3: Example of MTF acquisition with the IQI

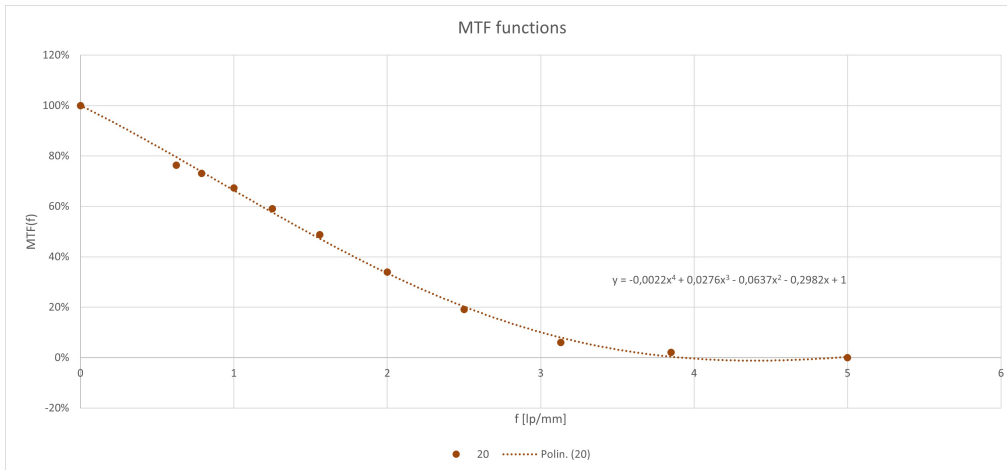


Figure 5.4: Example of measured MTF, 1.5 mA at 180 kV for medium focal spot, $M=1.24$, or at 20 cm from the Detector, $f(10\%)=2.99$

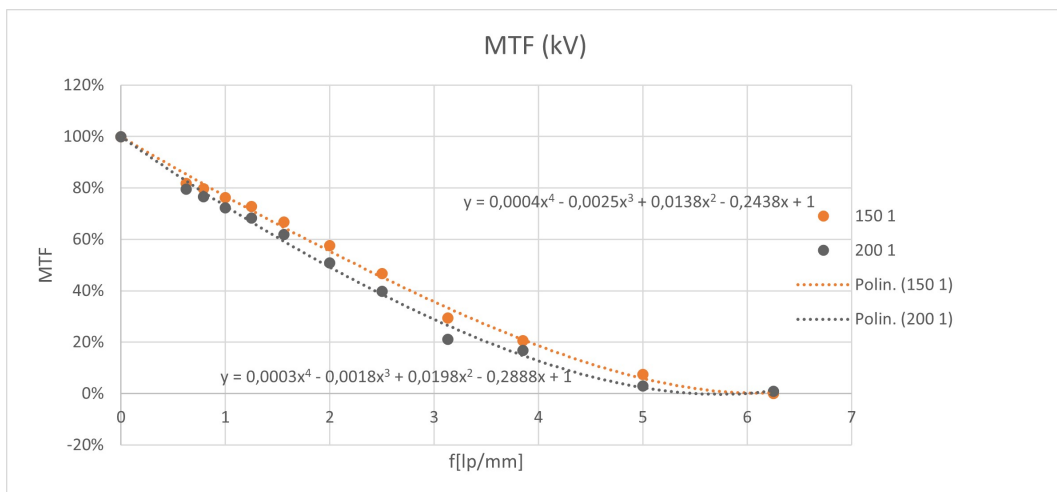


Figure 5.5: Effect of kV increase on MTF

blue curve does not have the highest frequency point considered, since the previous one was identically zero due to the impossibility to distinguish the formed peak in the gray values scale. Consider it leads to a worsening of the interpolation that can even bring instability of the solver used to find the frequency associated to the required MTF values.

Effect of mA increasing

Increasing the mA has to be taken with some care. In fact, if we approach the saturation of the Detector, the MTF worsen, as shown in 5.6 and the information on the system imaged is completely lost in the saturation region. If saturation is avoided, increasing the mA leads to an increase of the MTF.

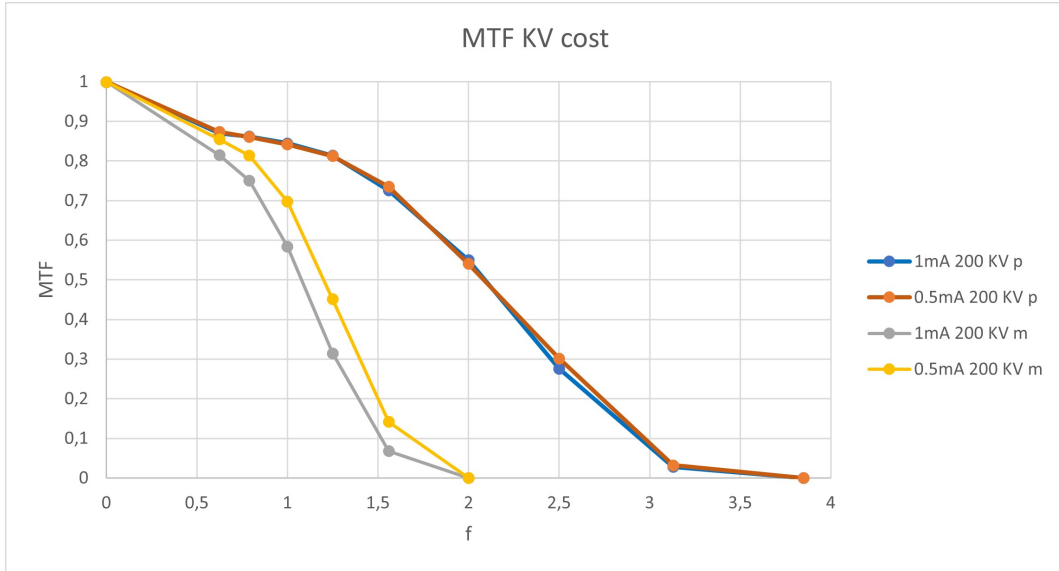


Figure 5.6: Example of measured MTF, double focal spot, effect of mA variation at 200 kV.

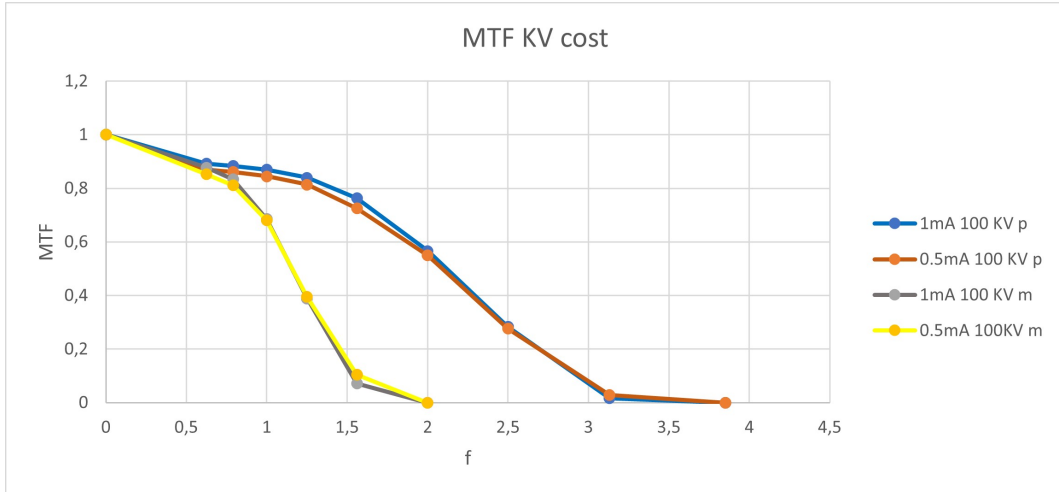


Figure 5.7: Example of measured MTF, double focal spot, effect of mA variation at 100 kV, half of above.

5.2.2 MTF as a function of magnification

the MTF changes with the magnification, as discussed in [15]. This fact is due to different relative weight of focal spot dimension and pixel dimension on the spatial resolution at different distances. We can calculate the expected optimal distance using a classical geometrical optical approach, imposing that the geometrical penumbra must be equal to half of the pixel dimension, using the nominal focal spot dimension.

$$PS/2 = \frac{DDO}{DDF - DDO} * FS \quad (5.1)$$

Where PS is the pixel size, DDO the distance between detector and the object, the IQI, and DDF is the distance between detector and the tube.

After that, it can be compared to the experimental measures to obtain the observed dimension of the focal spot. These measures require constant mA and kV, since different kV or mA, as discussed above, change the interaction with the IQI, changing the result of the measures. The results will be presented in the following chapter.

5.2.3 MTF with tube filtration

It is interesting to observe the effect of posing a filter right after the tube and observe its effect on MTF. This was done with a 0.3 mm copper filter, and the result provided that the observed focal spot is increased. This can be understood thinking about the interaction of the radiation with the filtering material. It is dominated by photo-electron absorption, but Compton scattering cannot be neglected, and this effect provides a widening of the equivalent focal spot, that is the focal spot dimension seen by the object-detector system, considering tube and filtration as a whole.

Results are presented at the end of the following chapter and discussed in more detail in the chapter 7.

Chapter 6

MTF measures for Focal Spot characterization

Focal spot, as above discussed, is one of the main characteristics of the imaging system. When a component has such an importance in a system, two fundamental questions must arise in the mind of an engineer or technologist:

- How do I test if the declared parameters are met by the system I bought?
- How do I verify performance of my component, to understand if I have to change it or it is still in nominal or acceptable performance?

The following methods can answer to these questions, but they have different pros and cons that will be discussed. The Frequency ratio method is completely new, the optimal magnification method is an interesting application of geometric optics principles and MTF measures, combining the two into a solid method of analysis. Some practical application of this second method will be described in detail, since they were tested directly.

6.1 Classical methods

Classical methods that can be used rely on the possibility to show directly the form and dimensions with a given magnification of the focal spot. The most used is the Pinhole camera, however other techniques can be exploited, such as the slit camera imaging.

6.1.1 Slit camera

The slit camera method makes use of a metal plate with a slit, that let x rays pass and reach a dental plate. The exposition usually lasts some seconds, depending on the settings and the nominal parameters of the imaging system. Two acquisitions have to be made, since the focal spot can be of different dimensions along the two axis.

Once the dental plate is imaged, it can be developed and it shows exactly a



Figure 6.1: Image of a plated impressed by means of a slit camera method.

magnification of the focal spot. Knowing the distance between the slit and the plate from the tube, the magnification can be calculated, and it enables to calculate the focal spot from the measurement of the shadow on the plate. The index of consumption can be deduced by the vanishing effect on the impressed zone, along with the increased dimensions, but its quantification is really operator-dependent and rely most on the experience of the operator, as can be seen in 6.1.

This method can be used to understand if a strong degradation is occurring, but it cannot be exploited to understand properly what the conditions of aging of the focal spot are.

6.2 Frequency ratio

The Frequency ratio is a method that tries to exploit the correlation between the focal spot dimension and the MTF. It is able to perform a comparison between two focal spots based on the ratio of their frequency values at a given MTF value, with the same kV, mA, exposure and integration settings. It is fast as method, since it does not need the acquisition of multiple MTF measures, or to mount special supports on the tube. In the following, the reference value for MTF will be the 10%.

If a reference focal spot is used, it can be tabulated along with the initial value

of the ratio for a given focal spot, and then it can be evaluated its grade of degradation.

It is a procedure requiring at most a couple of tens of minutes if an adequate positioning, pre-heating and parameters check is performed. It can be performed with just the IQI and the polystyrene support, it is not affected by flexion of the supporting system and errors of positioning due to mechanical adaptation of the support. In fact, It is not require to adapt the mechanical support to the tube, so can be performed without any special devices and by anybody, since it does not require any specific training and can be easily standardized and automatized.

Its main drawback is that the ratio between the MTF values can vary sharply with the settings if the two focal spot have quite different dimensions. This require using a reference focal spot that has dimensions as close as possible to the inspected one, so that dependence on parameters is minimized. This should lead to higher stability of the method. Since there were available just two focal spots and that testing time was of the order of a few months, on a system that works no longer than few hours a day, it was not possible to test direct degradation of the two focal spots, so comparison with a third focal spot was not possible.

6.2.1 Effect of parameters on FS ratio

The effect of changing the parameters was analysed to understand the stability of the method with respect to fluctuations or errors not revealed of mA or kV output or positioning errors of the IQI. What was found is quite interesting. Changing the values of kV 6.2 or mA (compare with 6.4 and 6.3), the trend of the Frequency ratio is parabolic, and the stationary point is reached within the inspected range of inspection of the parameters.

This allows us to select the value of the stationary point to minimize the fluctuation associated to unrevealed changes in the parameters. The parabolic trend shows that the effect of kV and mA on the MTF does not follow the same relation for the two focal spots. This fact is the outcome of different effects regarding the interaction with the IQI material and the effect on the focal spot dimensions of different parameters.

The parabolic trend is not a negative feature by itself, since the stationary point can be exploited for stability.

However, there is another effect that is not positive at all. If we change the positioning of the IQI, we can see that the coefficients of the parabolic interpolation changes dramatically, they can even change sign, as shown in figure 6.5. So, it is requested that the positioning has to be accurate and precise. It is not a strict requirement, but it is good to know what the limitations of our approaches are.

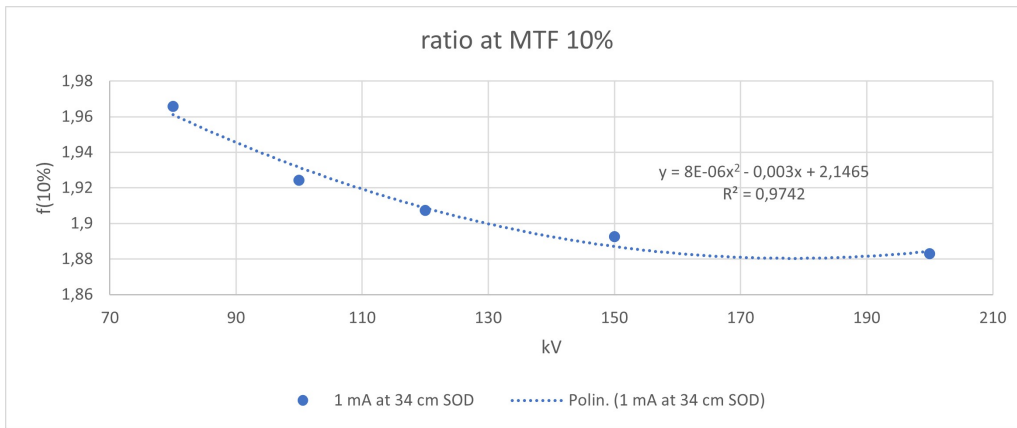


Figure 6.2: Trend of the Frequency ratio at MTF=10%, with $M=3.088$, or at 34 cm distance from the source, as function of the kV, 1 mA

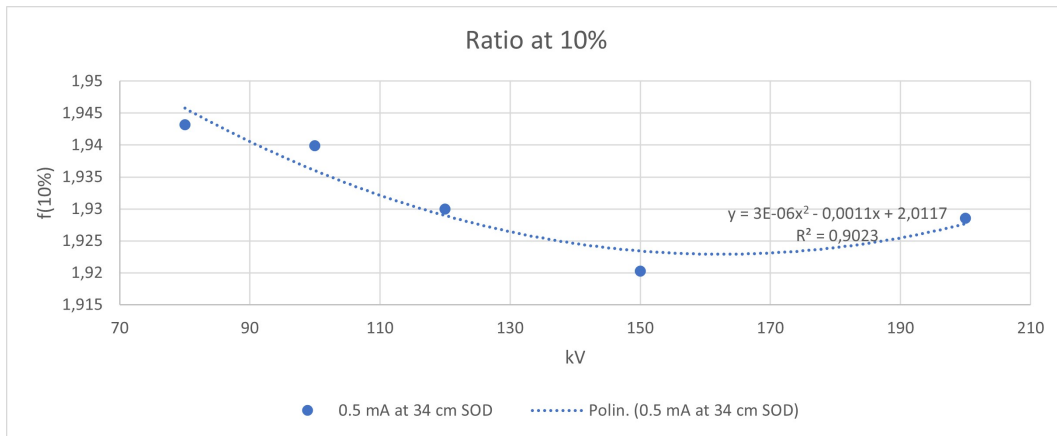


Figure 6.3: Trend of the Frequency ratio at MTF=10%, with $M=3.088$, or at 34 cm distance from the source, as function of the kV, 0.5 mA

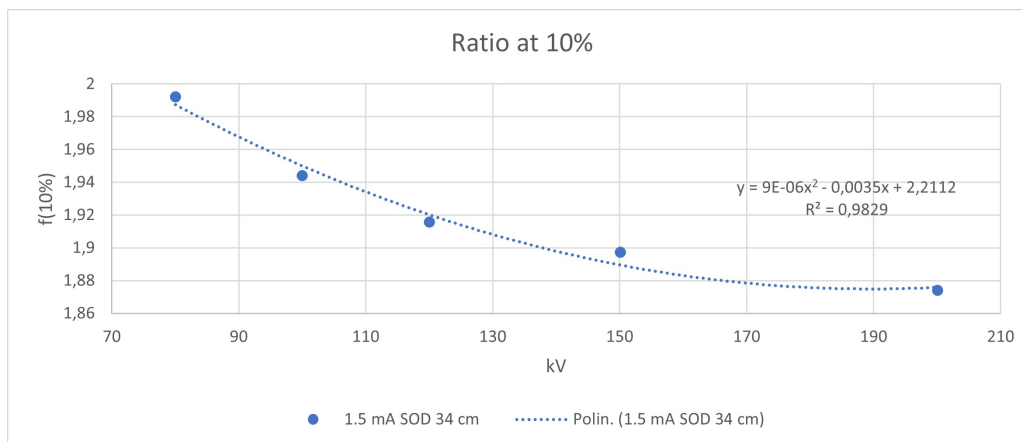


Figure 6.4: Trend of the Frequency ratio at MTF=10%, with $M=3.088$, or at 34 cm distance from the source, as function of the kV, 1.5 mA

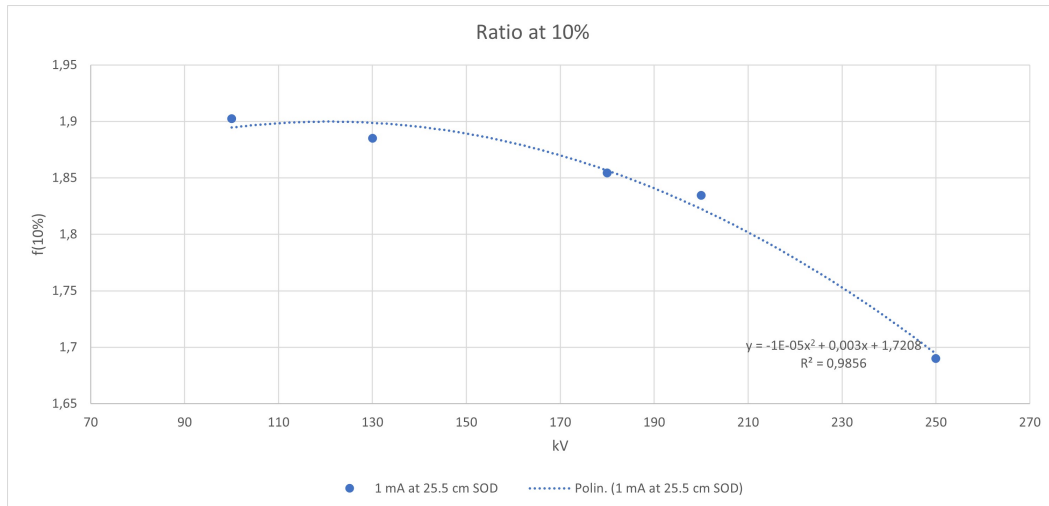


Figure 6.5: Trend of the Frequency ratio at $MTF=10\%$, with $M=4.118$, or at 25.5 cm distance from the source, as function of the kV, 1 mA

6.2.2 Use of the ratio

As already discussed above, the Frequency ratio method is powerful, but it has to be used knowing its sensitivity to parameters, since it is not robust with respect to unexpected changes without counter measures. However, fixing all of the usual parameters and creating a reference, it is easy and fast to correlate the dimensions of a focal spot to a reference one. To increase the stability of the method, it is possible to characterize the Frequency ratio changing slightly the parameters, in order to estimate a possible order of magnitude of the errors.

6.3 Optimal magnification method

This method is quite laborious to be performed, it requires accuracy in positioning the IQI and in measuring the distance from the source. This was quite a complex point, since the measures were performed with an electrician meter, in balance in order to not to touch the IQI support and the mechanical system of the central plate. Thus, errors in the measuring can occur, in the range of ± 1 or 1.5 cm, since that was the difference that was observable in performing the measurements, depending on the stability of my positioning.

Nonetheless, this measure can be automatized using the positioning of the plate by the movement system, and this method will become rock solid.

To calculate the equivalent focal spot from the measurement of magnification associated to maximum MTF value, the geometrical optics concept of shadow and penumbra were exploited.

FS [mm]	M_{opt}	DOD [cm]
1	1.10	9.55
0.4	1.25	21

Table 6.1: Comparison between Focal Spot (FS) dimension, optimal magnification and Detector Object Distance (DOD) in this system

6.3.1 Theoretical calculation: geometric optics

The formula to be exploited is the 5.1. This formula links the half size of the pixel to the focal spot, via the optimal magnification.

In order to find the optimal magnification, the MTF was exploited. The maximum value of MTF is assumed to occur at the optimal imaging magnification position.

What was found is coherent with what observed with the slit camera, that both the focal spots are still in nominal conditions, even if one may be slightly consuming. We are going to discuss it in more detail.

The calculations provide the results reported in table 6.1.

The results are calculated using a Source Detector distance of 105 cm, 0.2 mm of pixel size and the nominal focal spot dimensions. .

6.3.2 Measures of magnification

We are now going to discuss the measures performed. What was thought was to correct the calculations with the measurements in the first place, in order to compensate for the approximations introduced with the optical geometric assumption. However, it required both a more precise distance measurements and tubes that were not be used in extended way.

The observed functional behaviour of the function MTF(M) vs SOD can be exploited to estimate the focal spot dimension, since the behaviour of the MTF is quite sensitive to focal spot detriment.

In 6.6 the observed behaviour shows a maximum $M = 1.11$, or at 10 cm from the detector, to be compared with $M = 1.10$, or 9.55 cm expected from calculation. We have to consider that the distance measures were acquired in a way that do not guarantee accuracy to the cm values, we can suppose an esteem of error considering ± 1 cm in dimensional measurements for the medium focal spot and 1.5 cm for the smaller one, due to different positioning. The same calculations can be made for the case of small focal spot in 6.7, except that an uncertainty of 1.5 cm is used. This can be justified, because during the measurement, when I was closer to the detector, it was easier to find a support for my arm and to refer to the parallel, while it was harder when i was far from it and suspended completely. This resulted in an increased error esteem.

In table 6.2, we compared calculated FS from experimental data with nominal ones. Notice that a coverage factor of 2 is applied. We used the formula for

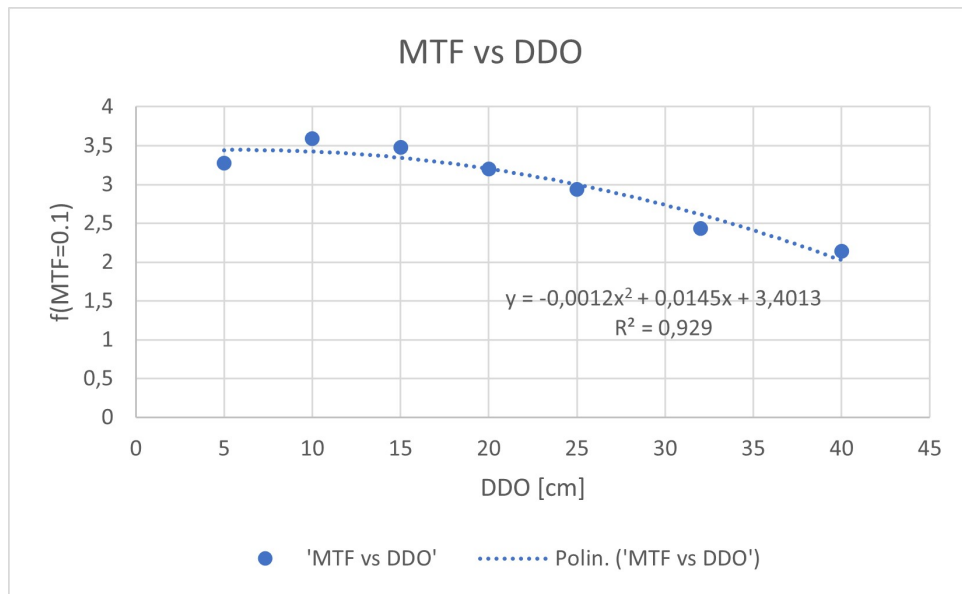


Figure 6.6: Observed behavior of MTF as a function of the distance between detector and object (IQI)

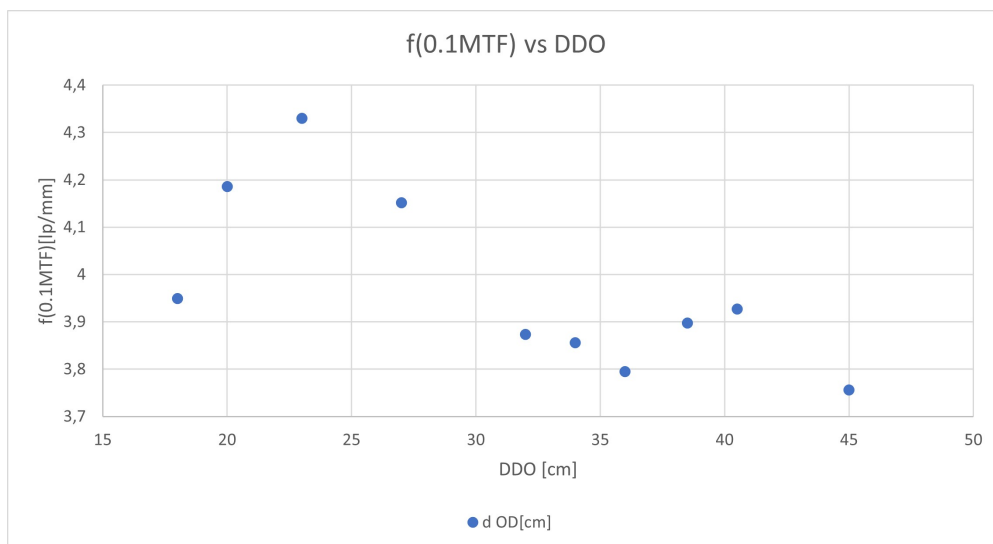


Figure 6.7: Observed behavior of MTF as a function of the distance between detector and object (IQI)

FS_{unc} [mm]	FS_{obs} [mm]	$FS_{nominal}$ [mm]
0.10*1*2	0.95 ± 0.20	1.00
0.019*1.5*2	0.357 ± 0.057	0.400

Table 6.2: Comparison between observed and theoretical calculations of the focal spot dimension for the two tubes

uncertainty propagation to calculate the esteemed error.

$$\sigma^2(X) = \left(\frac{dX}{dD}\right)^2 * \sigma^2(D) \quad (6.1)$$

The method is more precise for greater focal spot dimension. The measurements can be refined; however results are good and can predict the dimensions of the focal spot. If the error is reduced, the method could provide accurate esteem of the focal spot, and it can be performed in both dimensions to address the difference in the two dimensions of the focal spot.

Further considerations on MTF(M)

The study of the dependence of MTF from magnification, or equivalently distance from source or detector, can provide also an important information. If we consider performing a radioscopy or a tomography, the effect of magnification itself is usually negligible in the object. however, the MTF can change remarkably, so if we would like to perform with the finest spatial resolution, we cannot go in areas where the MTF is lower. Furthermore, if we perform an inspection of an object that is placed in a region where the slope of the MTF curve is accentuated, we are going to under-perform since the lowest MTF value will affect the image. It has to be taken into account for refined images.

6.3.3 Effect of filtering on FS dimension

Let us see an application of this method, able to quantify an interesting effect of the physical filters used at the source: the equivalent enlargement of the focal spot.

It can be seen as a detrimental feature of the filters applied at the source, but it is what makes the difference with respect to detector filtration and makes it even better in any considered case in this thesis.

In 6.8 we can see two effects typical of the filtering procedure. The first is easily predictable, consisting in a global lowering of the MTF values. What was not expected was the translation of the position of the maximum. It passes, for the small focal spot, from observed 23 cm DDO, or $M = 1.28$ to 20 cm, or $M = 1.24$ in case a 0.3 mm brass filter is applied to the tube. It results in an equivalent focal spot greater than the former without filter. The benefits of the filter will be analysed in the following of the thesis.

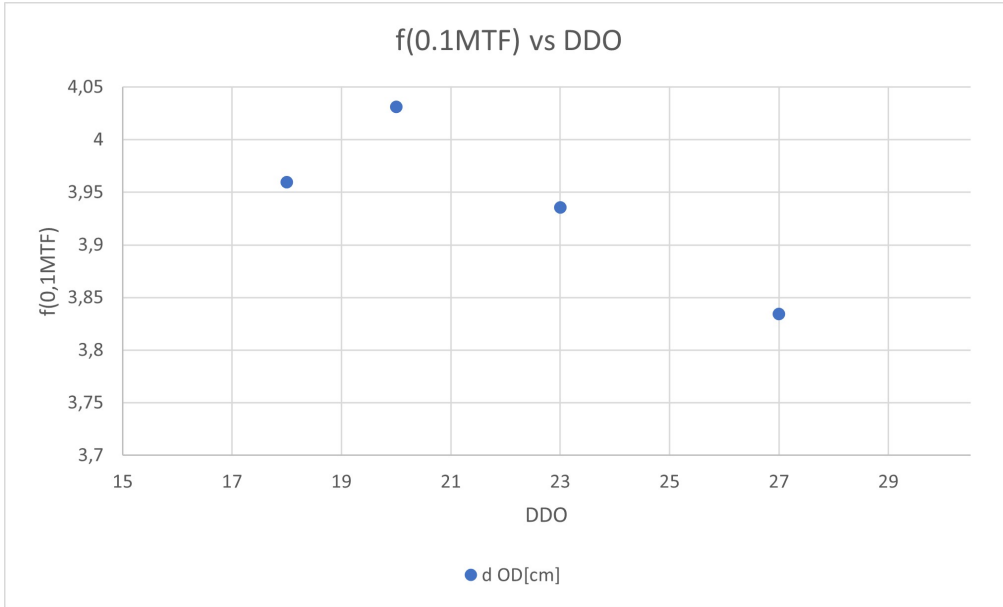


Figure 6.8: Behavior of MTF vs DDO with an applied filter of brass, thickness 0.3 mm

FS_{former} [mm]	FS_{filt} [mm]
0.357 ± 0.057	0.425 ± 0.075

Table 6.3: Comparison between Focal Spot dimension with and without pre-filtering

Chapter 7

Application: Brass filter

7.1 Effect of filtration on tube and detector

The effect of filtration is used to change the energy spectrum outgoing from the tube. A study in medical applications is provided in *The Influence of X-ray Spectra Filtration on Image Quality and Patient Dose in the GE VCT 64-Slice Cardiac CT Scanner* [17]. From the point of view of attenuation, using the Lambert-Beer law (2.1), what we found is the independence of the intensity from the order of the faced materials. This is due to the exponential dependence of the attenuation. Following this reasoning, it can be wondered if filtering at the source or at the detector can make any difference, mainly in terms of scattering attenuation.

This evaluation was made once again exploiting MTF measures.

7.1.1 Tube vs Panel filter

There are two experiments that provides useful insights to the difference between filtering at tube and at panel.

Water imaging

It is worth analysing first a case study that has one specific feature: the sample contains water. Water is a compound capable of producing a high amount of scattering, both Compton and elastic, due to its small value of z , in pure water being 8. There will be some impurities, however they are not in quantities meaningful to modify the experiment outcome.

There are two imaging modalities to test, in order to understand the contribution of scattering and the effect of filtering due to water:

- Imaging with IQI superimposed with the bottle;
- Imaging with IQI nearby the bottle or a water tank, but not superimposed.

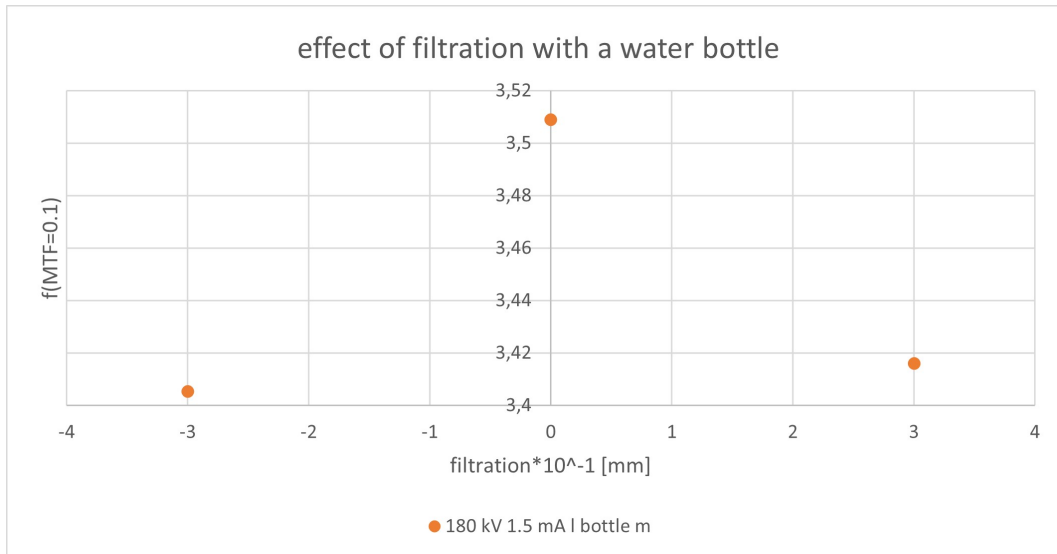


Figure 7.1: Effects of the presence of the water bottle near the IQI.

The bottle had a thickness of 10 cm, while the tank was 20 cm. The results show that filtering at the source is the most suitable way of applying a filtration.

In 7.1, it is clear that filtration is not convenient to be applied. However, the pre-filtration marked from the convention of + sign, gives smaller MTF degradation with respect to post filtration. Moving to 7.2, it is shown that $f(0.1)$ increases slightly, so the MTF raises, with pre filtration, and lowers remarkably with post filtration. In the last case, considering the presence of the water tank 7.3, pre-filtration remarkably increases $f(0.1)$, while post filtration reduces slightly once again.

Explanation

What was not considered in the previous reasoning is that an additional effect of pre-filtration exists: it is produced, as we saw in chapter 6, an equivalent enlargement of the focal spot. This effect produces just a lowering of the contrast in post filtration, while in pre-filtration contributes to remove from the beam rays that while undergo scattering inside the object. Opening up the beam, the angle that is required to reach the detector area imaging the interested object area by rays far from that point of interaction is increased, and then the probability of this event to occur is significantly lowered.

Iron imaging

The second experiment is realized using 1 cm thickness iron. The experiment is particularly important, due to the fact that iron can produce de-excitation x rays due to photoelectric effect and it is interesting to understand the impact

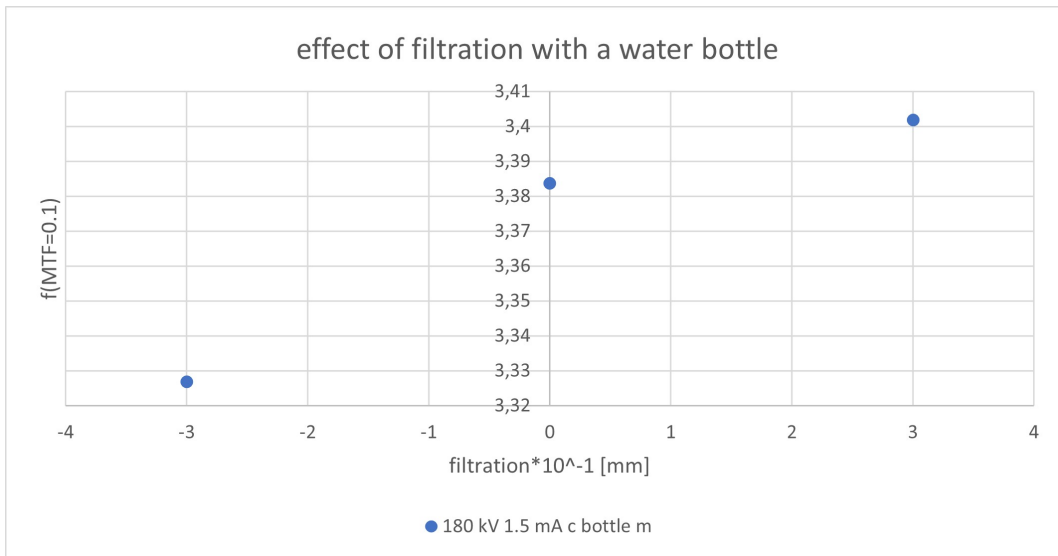


Figure 7.2: Effects of the presence of the water bottle placed in front of the IQI.

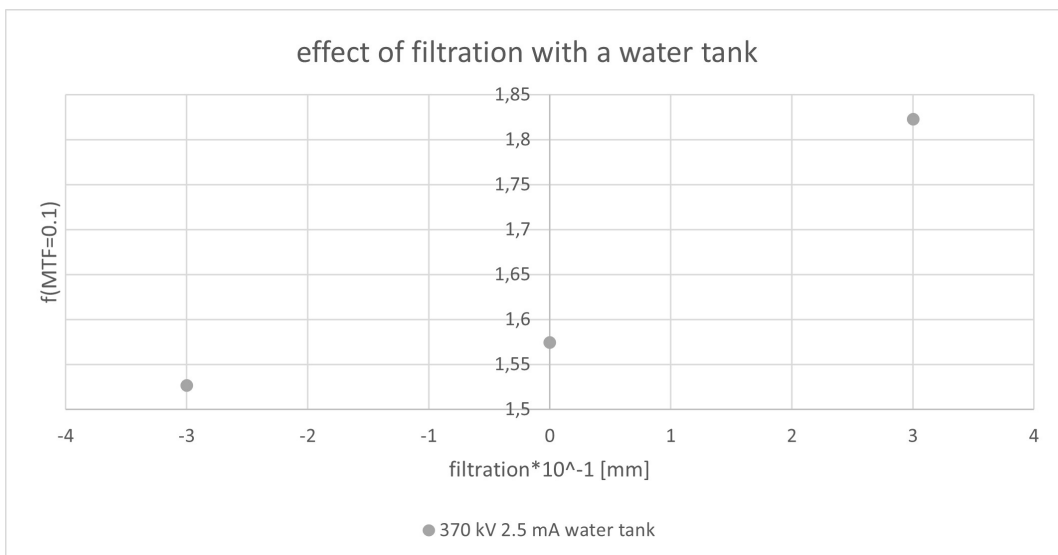


Figure 7.3: Effects of the presence of the water tank near the IQI.

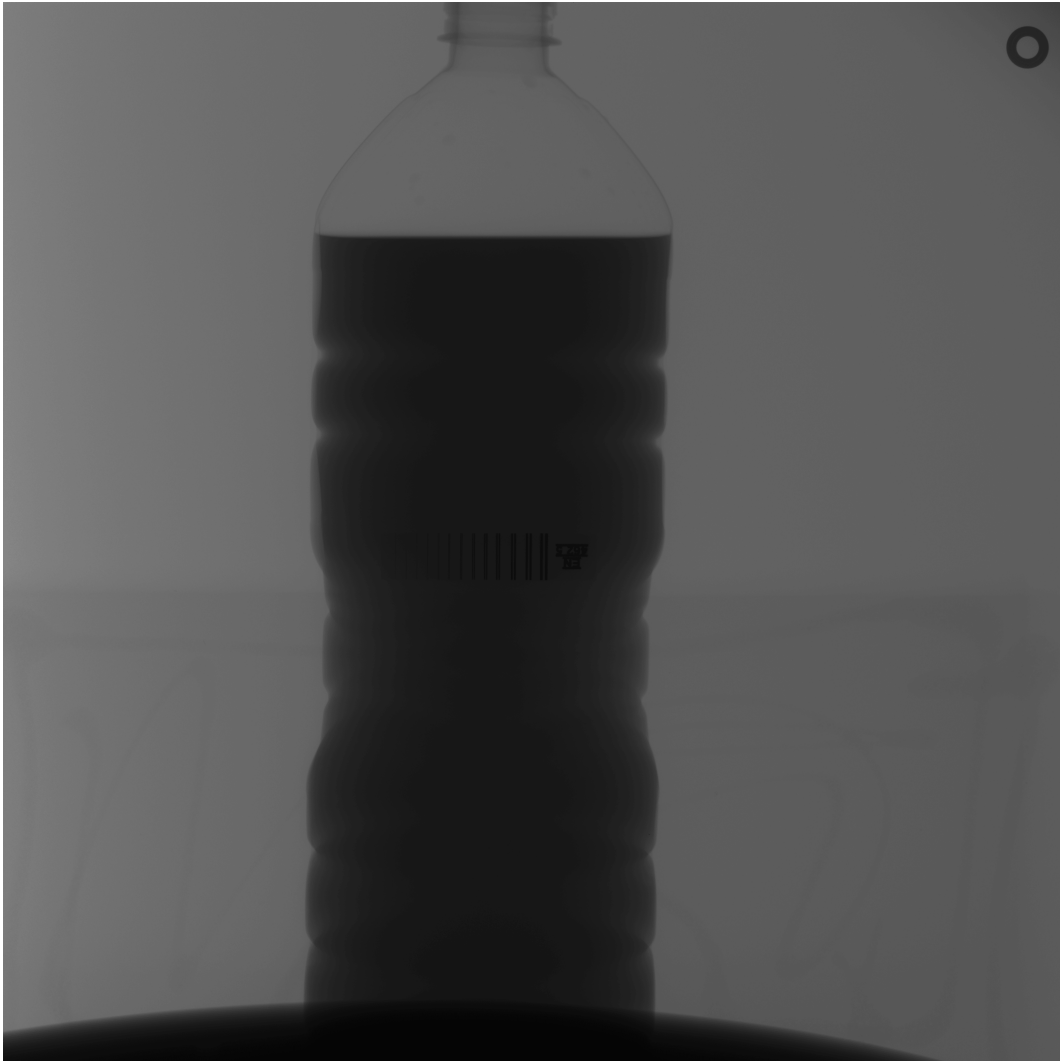


Figure 7.4: Imaging of a water bottle in central position with 0.3 mm brass pre filtration at 180kV, 15mA at 90cm SOD, or $M=1.17$.

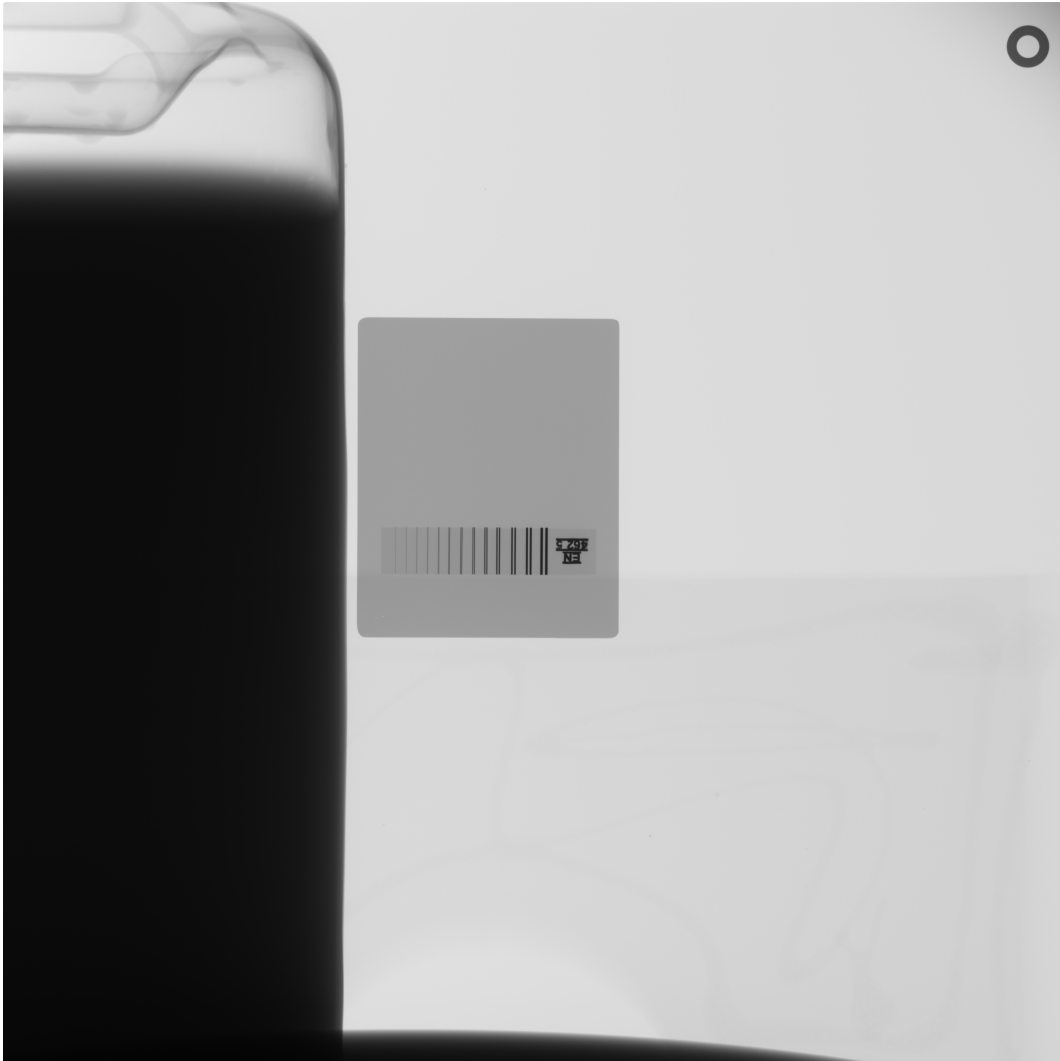


Figure 7.5: Post filtration of 0.3 mm brass with tank near the IQI. Parameters are 180 kV, 15 mA, 90 cm SOD, or $M=1.17$.



Figure 7.6: Pre filtration of 0.3 mm brass with tank near the IQI. Parameters are 180 kV, 15 mA, 90 cm SOD, M=1.17.

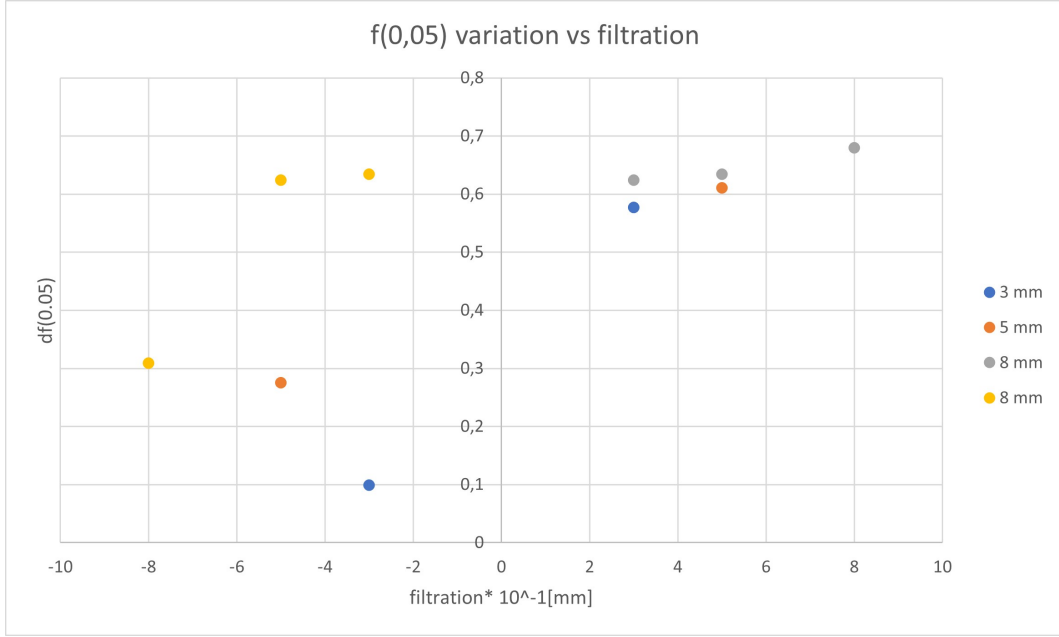


Figure 7.7: Effect of filtration on imaged 1cm exploiting $f(0.05)$ variation referred to not filtered image. + sign refer to pre-filtration, the same color represent same total filtration. Imaging is performed at 350 kV and 2.5 mA, medium focal spot is necessary to produce enough power output, SOD is 99 cm, $M=1.06$.

they have on noise. If their contribution is important, post filtration should provide good increase in Δf with respect to the reference. Nonetheless, being iron a material with a Z value quite high, photoelectric effect should dominate the interaction, lowering scattering importance and reducing the difference between pre and post filtration. What is obtained is the plot 7.7, which allows to make some important considerations. First of all, it is evident that, considering increasing filtration on one single side, so considering blue point, then orange point, an lastly the higher single-side filtration point, pre-filtration doesn't show a strong gain in Δf increasing further the filtration, while post filtration requires an higher thickness to saturate the effect. Second consideration is that, with same total filtration, pre-filtration provides a gain that is at least double the one provided by post filtration. Then, it is analysed the contribution provided by a mixing of pre + post filtration. It can be seen considering the value of single-side filtration and confronting it with the same amount of single-side filtration with a higher total filtration. What is found is that post filtration gives a small increase in Δf , and the higher the amount of post filtration in the total filtration, the lower the Δf gain. Then it can be deduced that post filtration is not convenient in the analysed cases, since it never has shown to give better MTF results with respect to pre-filtration.

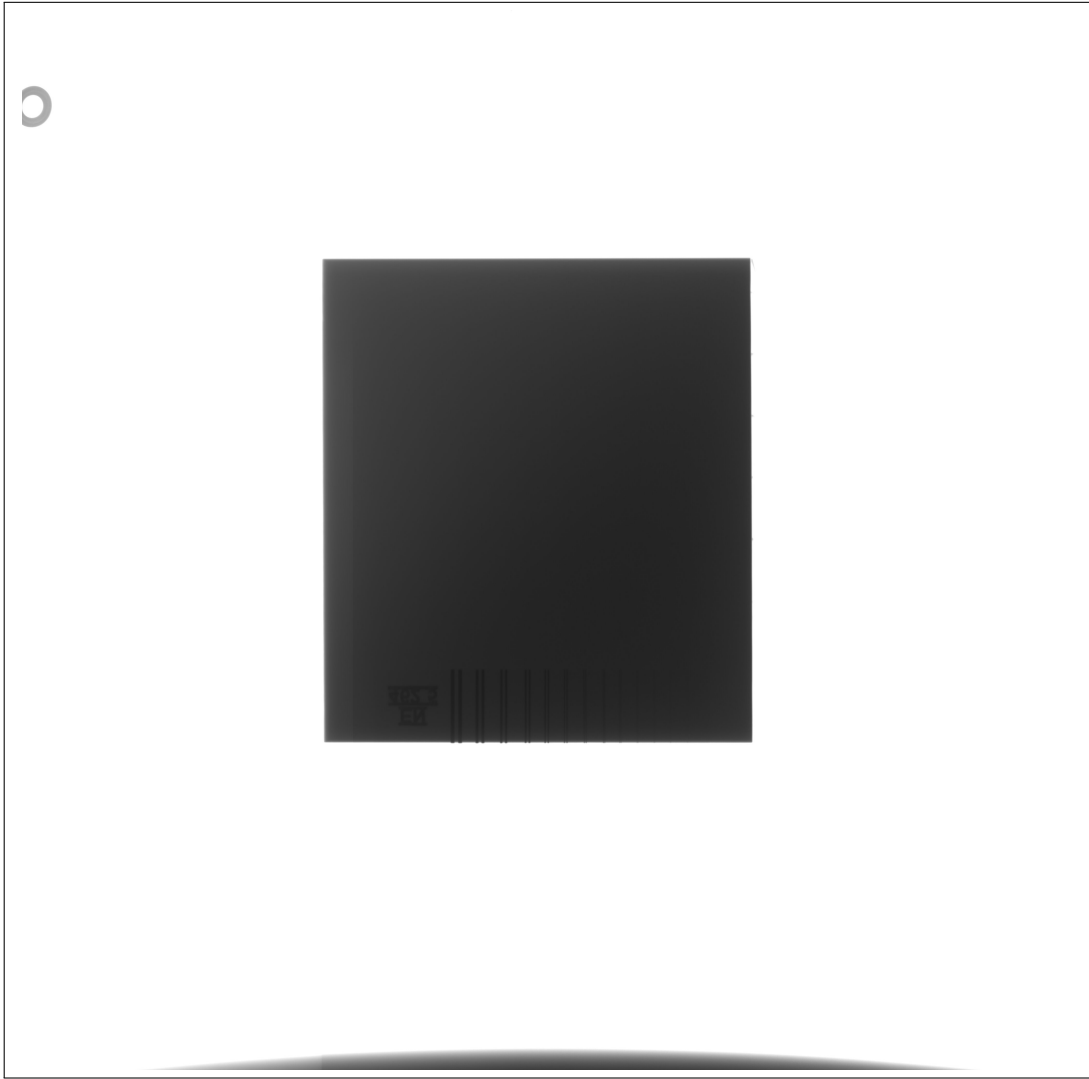


Figure 7.8: 1 cm Fe reference image, $M=1.78$

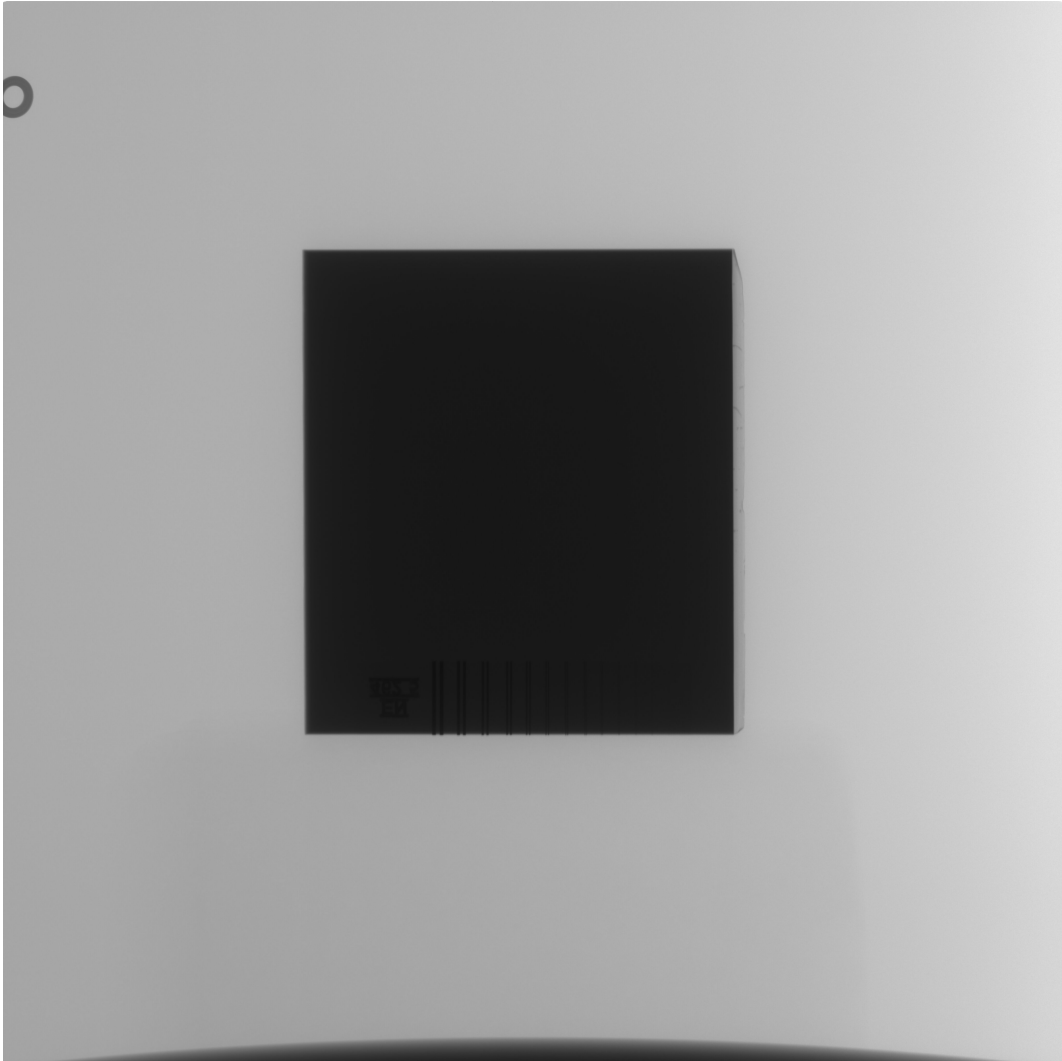


Figure 7.9: 1 cm Fe with 0.8 mm pre-filtering

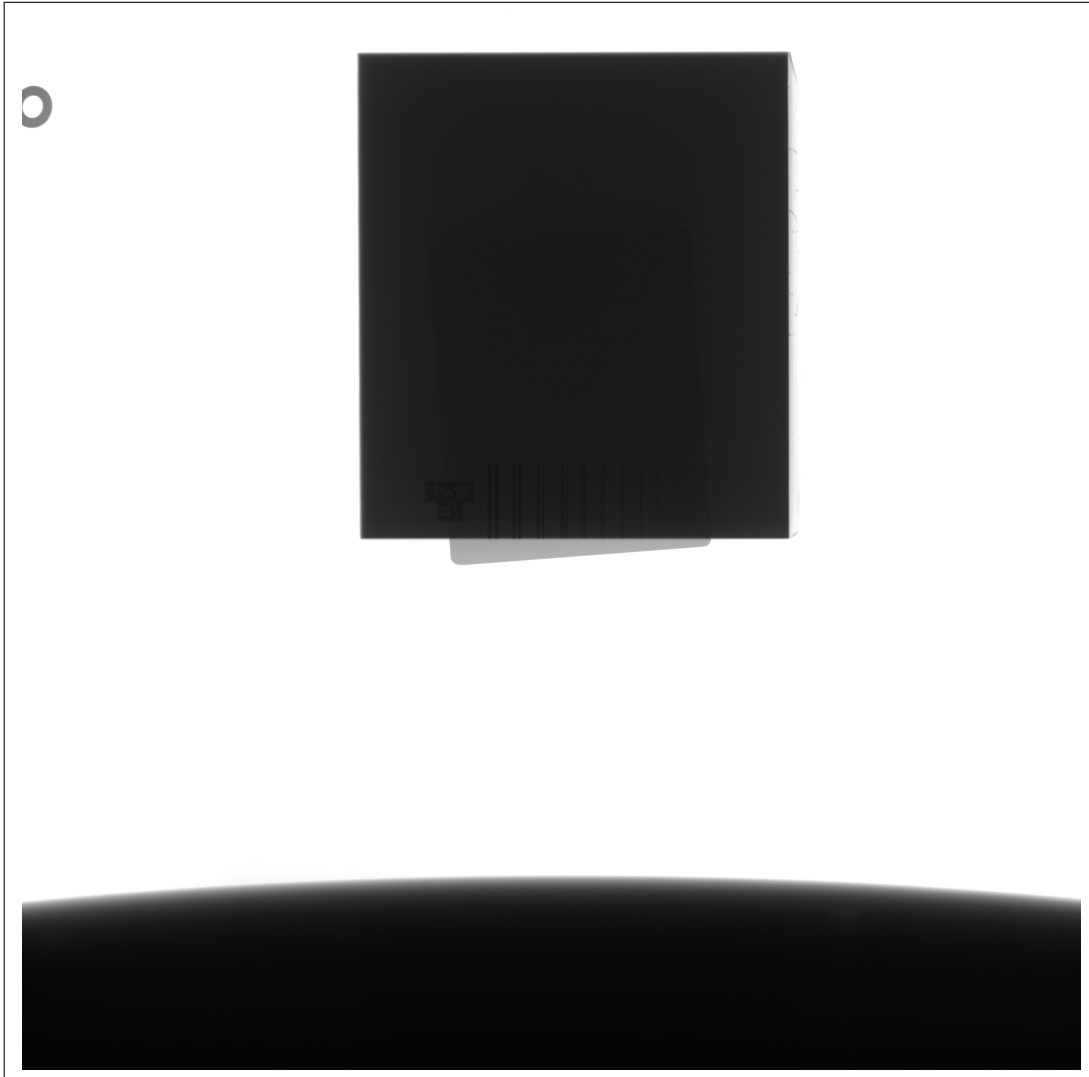


Figure 7.10: 1 cm Fe with 0.5 mm pre-filtering and 0.3 post filtering

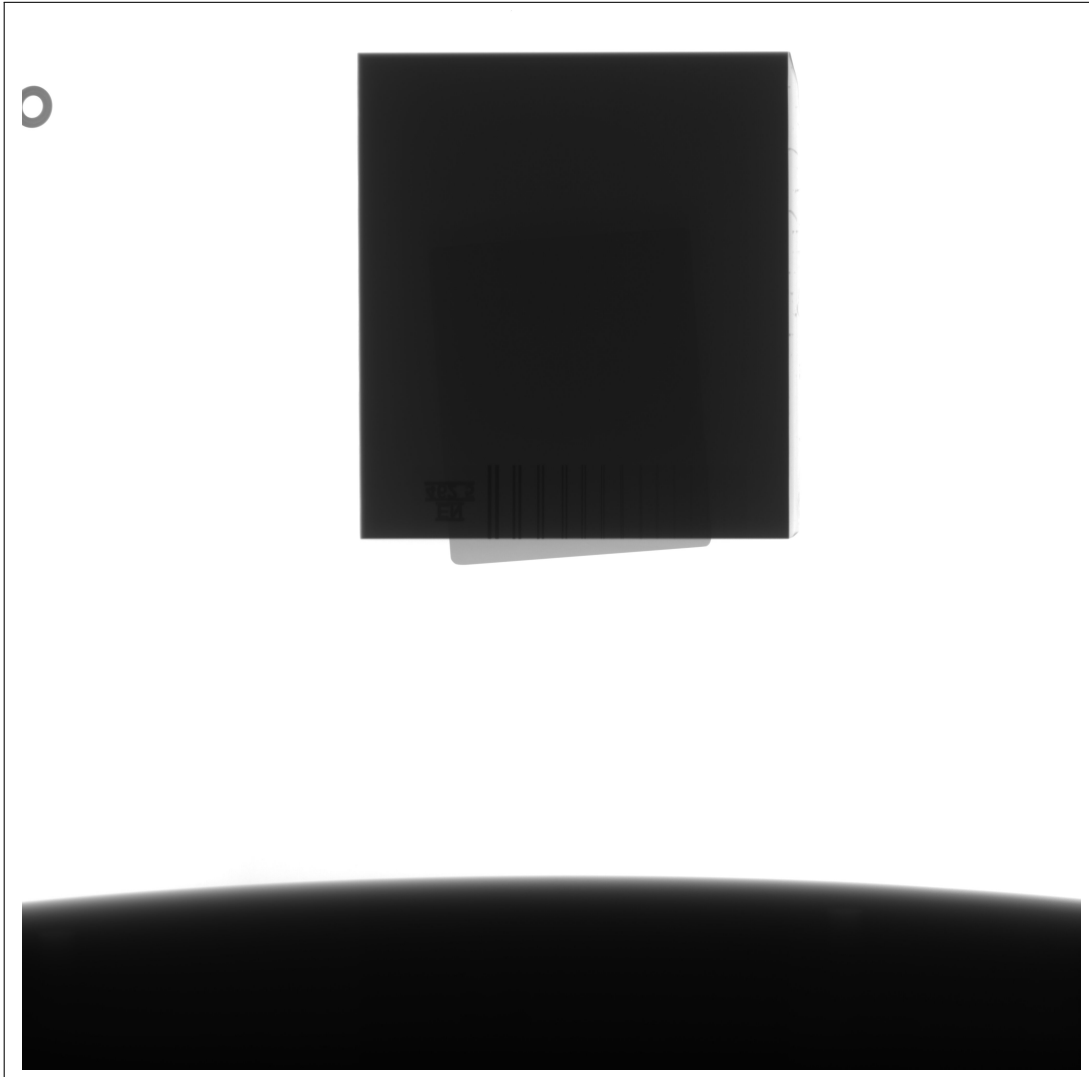


Figure 7.11: 1 cm Fe with 0.3 mm pre-filtering and 0.5 post filtering

7.1.2 Experimental maximization of MTF to find highest useful filtration

It will be shown that source filtration is the most effective way to operate filtration, that's why some evaluations were operated exclusively with source filtration, since detector filtration is not suggested in its use.

In order to understand the effect of single filtration, what can be done is to calculate, exploiting once again MTF measures, the filtration thickness providing the *maximum MTF*.

It is not the optimal filtration, because optimum does not include just contrast, but also noise and power output. The experimental values were acquired using an IQI certified by the ASTM and an object of iron. Parameters were 350 kV, 2.5 mA and 99 cm Source Object Distance (SOD), or $M = 1.06$ referring to the IQI, used to produce the values in table 7.1 that can be represented graphically as in 7.12.

Filtration was increased using the thicknesses available at the Company, they are the one reported in table 7.1, alongside with the increase in MTF from the baseline.

Thickness [mm]	MTF increase [$f_i(0.05) - f_0(0.05)$]
0.3	0,578
0.5	0,611
0.8	0,680
1.0	0,704
1.3	0,741
1.5	0,816
1.8	0,704

Table 7.1: 1 cm Fe MTF increase from reference with increasing tube filtration

The case of increased thickness and energy shows that the effect of filtration cannot be described as a square fit in all of the cases, as shown in 7.13. Here, 1.5 cm of Fe at 375 kV gives different results, for the single filtration, fact that will be described in the following, and for the filtration providing maximum MTF. Let us say that, in these two tests, filtration provides an increase in the MTF. Please notice that in 7.13 the exploited parameters is $f_{0.05}$ and not 0.1. This choice was made because of the strong attenuation provided by 1.5 cm iron plus the filtration at the IQI spatial frequencies.

The maximum MTF increase is not much greater than the surrounding values, meaning that the effectiveness of the filter in this application reaches a fast saturation increasing slightly the thickness. The uncertainty is not given for thicknesses, since they were measured before these tests and the instrumentation was not able to resolve for fractions of millimetre.

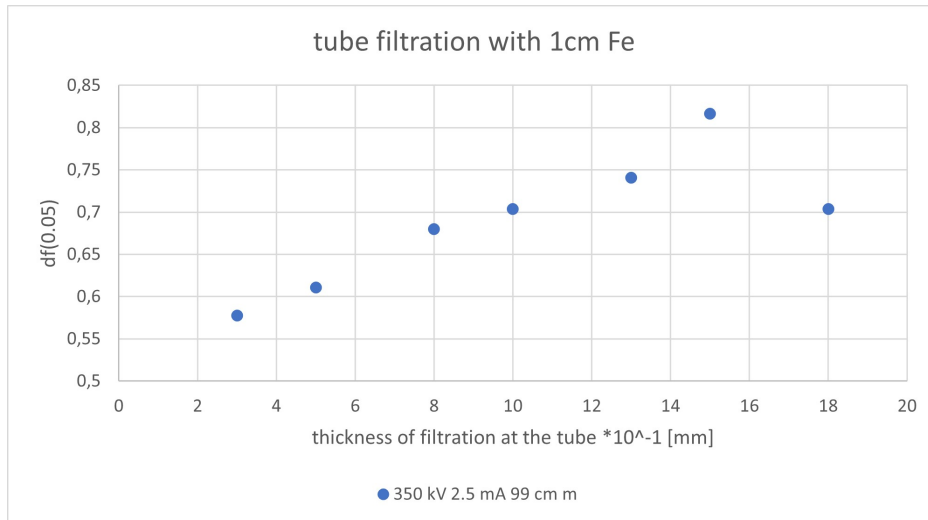


Figure 7.12: Graphical representation of MTF increase

Thickness [mm]	f increase [$f_i(0.05) - f_0(0.05)$]
0.3	0,679
0.5	0,541
0.8	0,683
1.0	0,696
1.3	0,791
1.5	0,850
1.8	0,849
1.88	0.888

Table 7.2: 1.5 cm Fe f increase from reference with increasing tube filtration

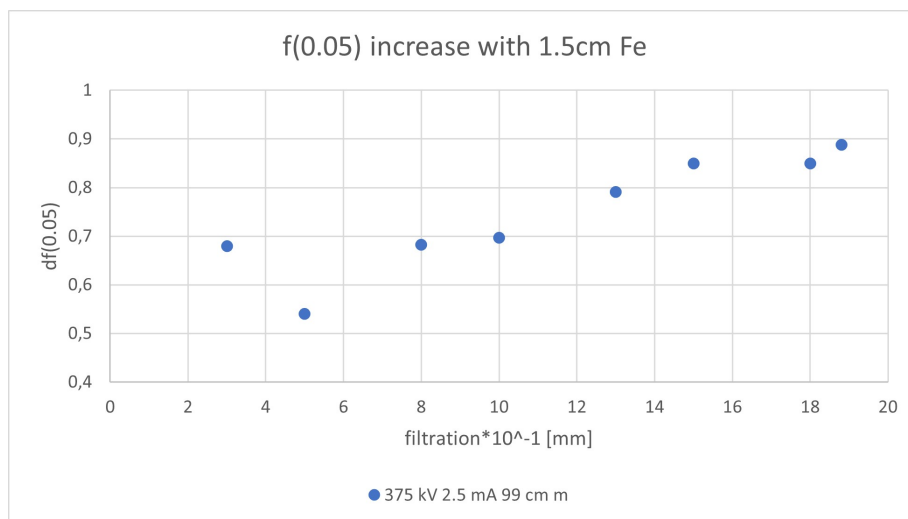


Figure 7.13: Graphical representation of f increase with increased thickness and kV

7.2 Material effect

The effect of filtration on different material is everything but negligible. It can be clearly seen looking at the following results, and the reason will be

explained in the following.

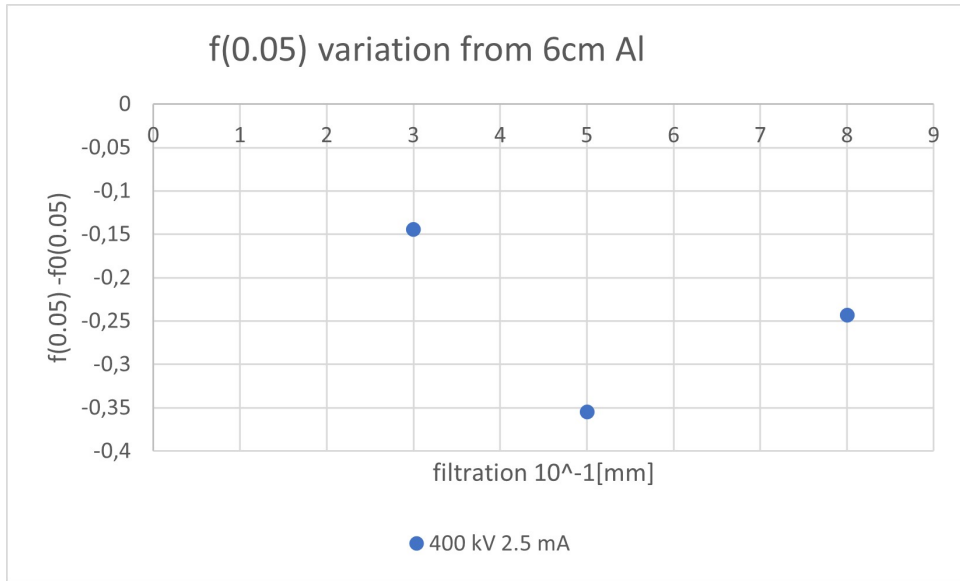


Figure 7.14: Variation of $f(5\%)$ with filtration, imaging 6 cm aluminium at 400 kV and 2.5 mA, to be compared with 2 cm iron, same parameters

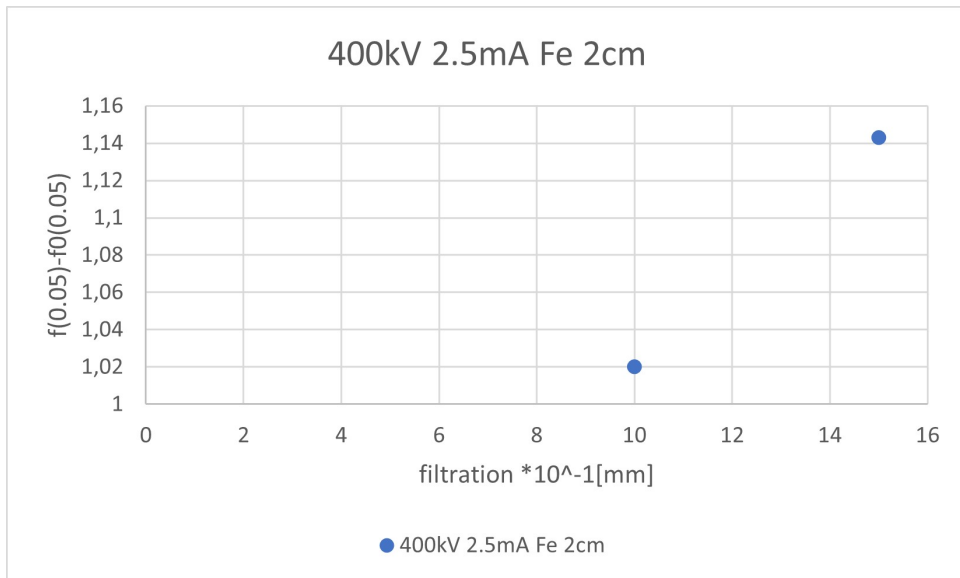


Figure 7.15: Variation of $f(10\%)$ of 2 cm iron imaged with 400 kV, 2.5 mA

In figure 7.14 and 7.15 it is shown that, at constant parameters, the values of Δf not only is strongly increased moving from aluminium to iron, but what is more significant is that they are negative per Al and become positive for Fe. The reason can be explained thinking at the effect of filtration on the spectral distribution. The cut-off point moves towards higher energies of the spectrum as the atomic number Z of the filter increases, behaving as a high-pass filter for the energies. This means that, as a rule of thumb, using a filtering material with an high Z compared to the one of the object to be analysed will filter

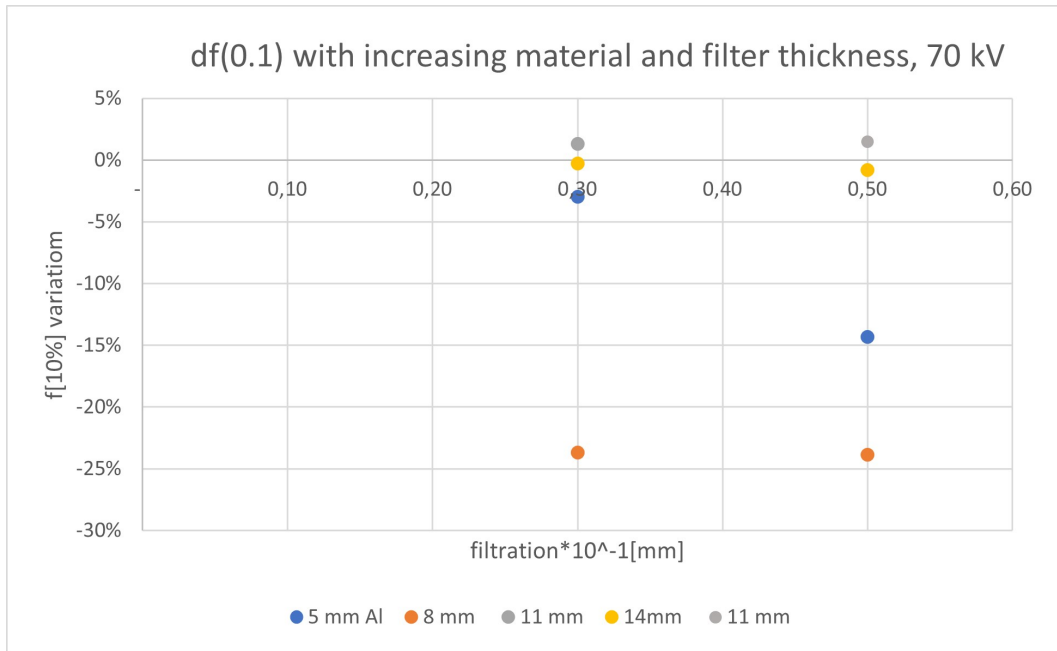


Figure 7.16: Effect of filtration with different thicknesses of Al at 70 kV, increasing filtration, according to percentile variation of $f(0.1)$.

too much, providing a decrease in contrast. It cannot be provided an absolute value for the Z to be used, since it depends also on filtration thickness and desired effect.

This can be observed also in the behaviour of the absorption cross section for different materials, understanding what the range of energies is where the cut-off occurs.

The benefits are obtained removing radiation that is not able to penetrate the material and can only become a source of noise due to scattering. In particular, diffraction effects at the edges can occur, producing an effect of nuance on them.

7.2.1 Thickness

The effect of imaging different thickness of the same material can be partially deduced by the discussion presented above, comparing two different thickness of iron. However, this discussion can be analysed in more detail, and also the case of different aluminium thickness is presented. Considering 7.16, We can see the effects of filtration and why it has to be understood when it can be used and when it shouldn't be used.

First, for the thinnest layers, 5 and 8 mm of aluminium, the contrast is worsened by the filter, due to cut of useful radiation. Then, at 11 mm, the percentile increase of f becomes positive, indicating that filtration provides a benefit to the imaging. Passing to 14 mm, the Δf decreases to zero or nearby, indicating that the filtration is absorbing useful radiation without stopping disturbances. If we compared now 7.16 and 7.17, we can observe that thickness of the filter

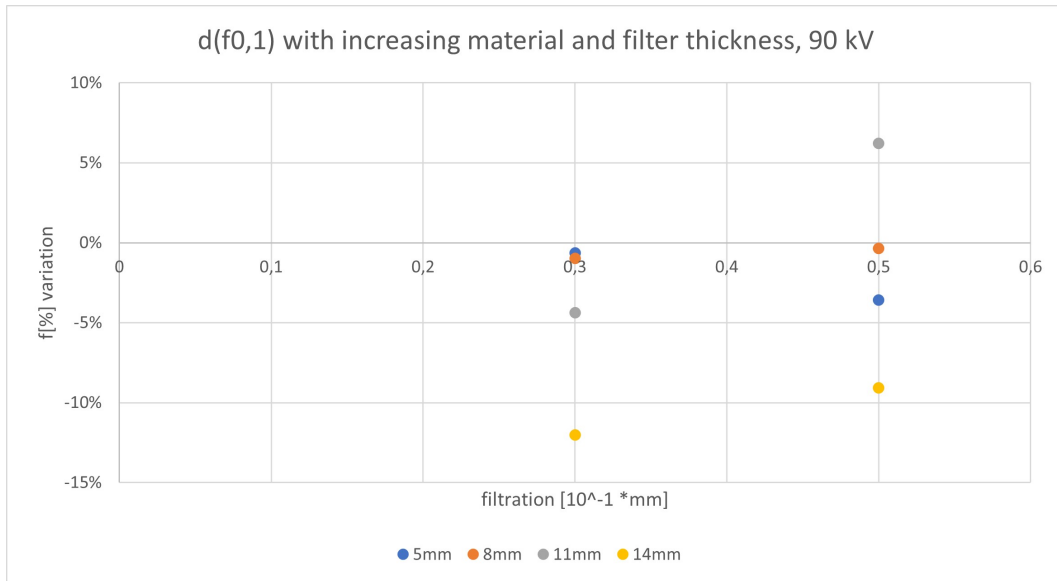


Figure 7.17: Effect of filtration with different thicknesses of Al at 90 kV, increasing filtration, according to percentile variation of $f(0.1)$

depend both on the particular thickness of the object and on the energy spectrum. It will be discussed in the following in more detail.

A different effect can be seen comparing 7.1 with 7.2. It can be seen that with an increased thickness of iron, increasing slightly the KV to compensate for stronger absorption, both the thickness of maximum MTF gain and the values if Δf increase. Then, it is expected that filtration can be more useful in case of thick and/or high-Z materials.

7.2.2 Energy spectrum

Spectral dependence of the effect of filtration can be deduced considering, as previously said, that the filter acts as an high-pass filter, and it is effective if it does not cut too close to the lowest energy of the spectrum that is able to reach the detector in a meaningful way. The discussion is complicated to be generalized for different reasons, the most relevant are two:

- X rays from X ray tube comes with non-uniform spectrum, with also characteristics peaks;
- Radiation has an exponential attenuation, so if we are far from object or filter edges of the X ray absorption spectrum, it is not sharp the cutting provided by the filter.

So, combining these two aspects can be really hard and probably Monte Carlo codes are the most straight way to a solution, even if they also bring with them other problems.

Looking at 7.16 and 7.17, it is observed that changing the voltage changes

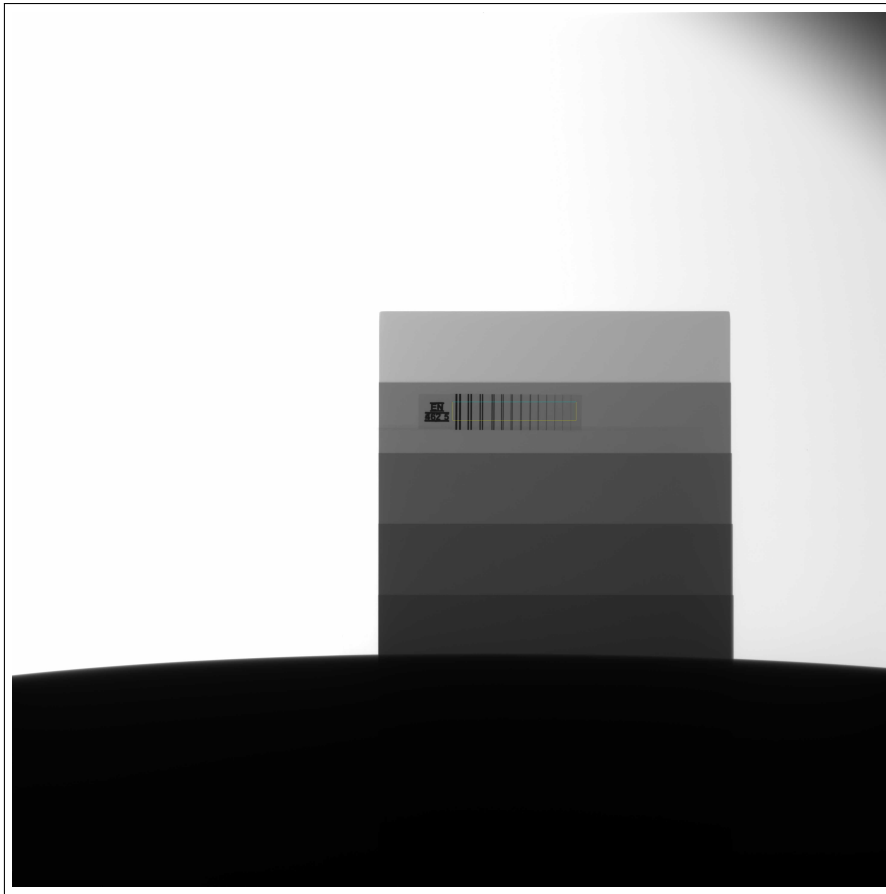


Figure 7.18: 5 different Al thickness, ranging from 2mm up to 1.4 cm, with 3mm steps.

what is the effect of the filtration. It can be said that optimal filtration is related to a specific material of the filter, a specific material of the object, its thickness and the chosen spectrum.

Comparing 6 cm of Al to 2 cm of iron, what can be observed is that, with the same energy spectrum and photon fluence, at the same positioning point, the effect of filtration is extremely different, going from totally negative with Al to outstanding with iron, supporting the hypothesis that energy spectrum has to be correlated with imaging material and then choose the filter to be applied.

7.2.3 Filtering material type

As mentioned above, the filtering type of material is brass in this thesis, but it can be of different materials and percentile composition, allowing to create interesting combination according to sharpness required and maximum absorption tolerated. The filtering material is not independent from the object, so it can be studied different type of filters for an object, that is good for a company that has a specific target material, but another convenient approach can be chosen to study for what kind of objects a selected filter provides improvements in image quality.

7.3 Non uniform materials

As a rule of thumb, experienced radiographers choose the kV in order to "pass" the thickest part of the material. This is done in order to be sure that radiation passes through all of the regions of the material, and mA and image post processing modify the visualization of the image. We can set a rule of thumb also for filtering material and thickness: *filtering that improves the MTF in the weakest absorbing part of the material increases the overall MTF*. This rule does apply considering a piece made of materials that have quite similar values of atomic number Z , bearing in mind the examples provided in 7.14 and 7.15 shown how the same filter, with different materials providing similar attenuation and with same kV and mA, provided different responses to the filter application.

This can be seen analysing the following case, in which two blocks of iron of thickness 1 cm and 1.5 cm are placed one near the other and imaged together. The effect of filtering is the increase of both the MTFs in the two regions, and the reduction of the gap between the two.

7.3.1 Imaging of 1 cm and 1.5 cm iron

This is a phenomenon that can be exploited in tomography, where it is almost certain that the pieces imaged will have different thicknesses in the rotation

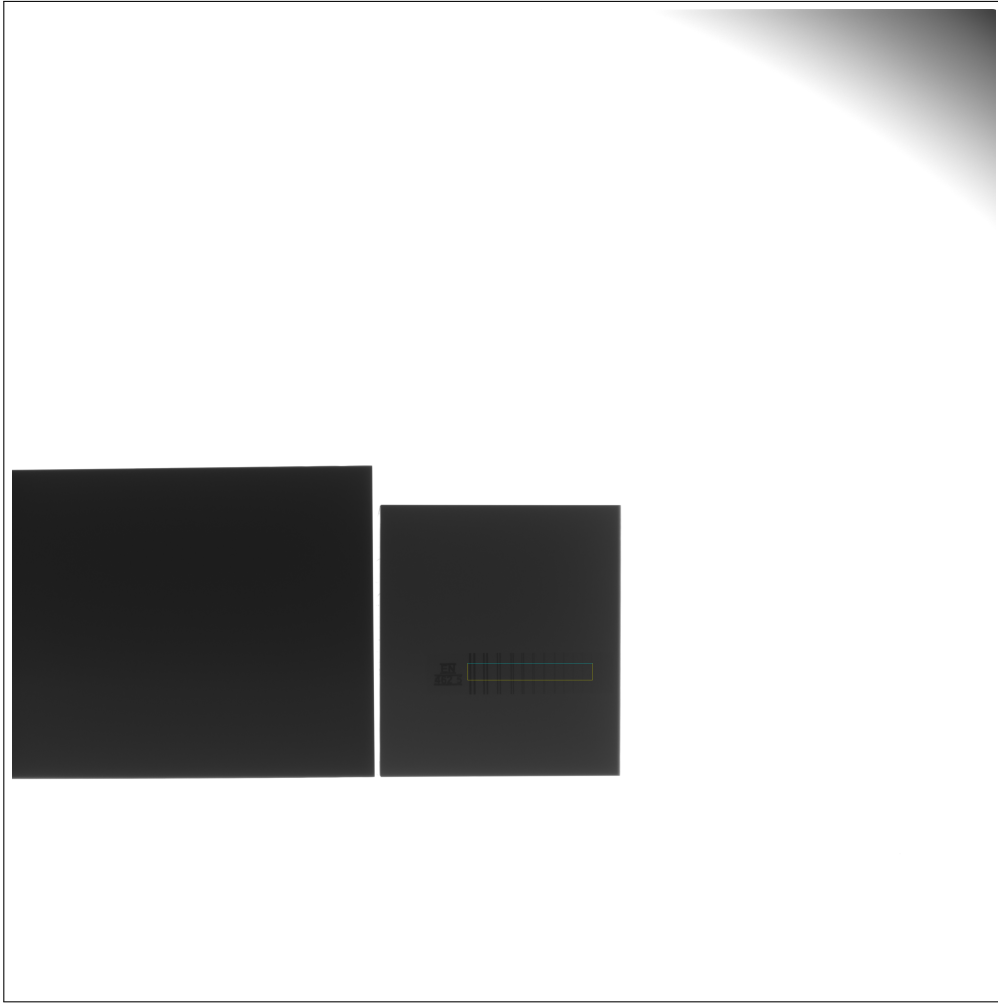


Figure 7.19: 1 and 1.5 cm iron imaged with 320kV, 3.1 mA at 100 cm distance from the tube, or $M=1.05$, focal spot of 1 mm, no filtration

projection direction but are usually made of quite homogeneous materials.

The imaging of two different iron thicknesses, namely 1 cm and 1.5 cm, shows clearly the above described behaviour. Looking at the MTF of the two regions, comparison is quite straightforward. The figure 7.21 shows that, introducing a filtration, the $f(0.05)$ in the region where it is lower is subjected to a stronger percentile increase. As already said, thanks to this effect, not homogeneous response can be attenuated, bringing a more uniform imaging of the different material thickness. The other effect, not analysed here, is that a filtration enables us to increase the energy used, or the mA, so the photon fluence, so that contrast is increased in the thicker region, but saturation in the thinner region is prevented. This result can provide better image quality with the same technology of tube, detector, electronics and mechanics and it is really low cost.

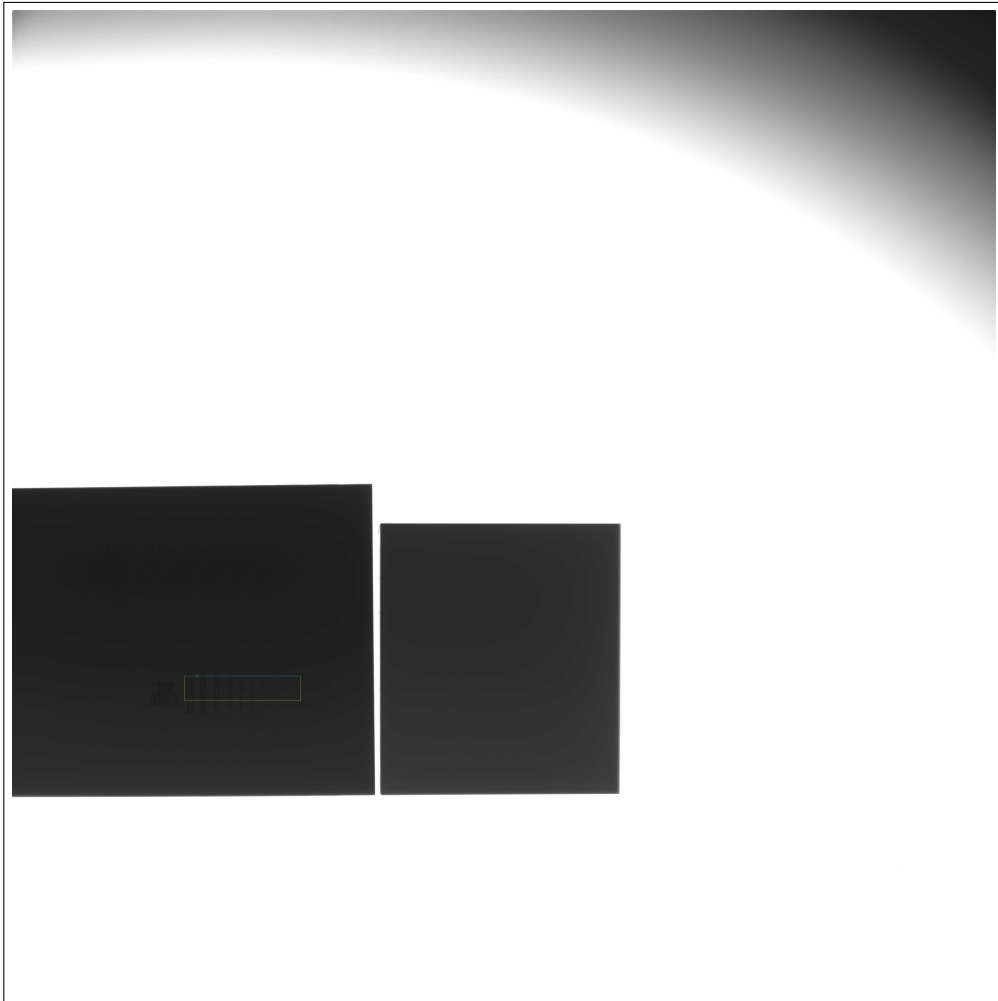


Figure 7.20: 1 and 1.5 cm iron imaged with 320kV, 3.1 mA at 100 cm distance from the tube, $M=1.05$, focal spot of 1 mm, with 0.5 mm filtration

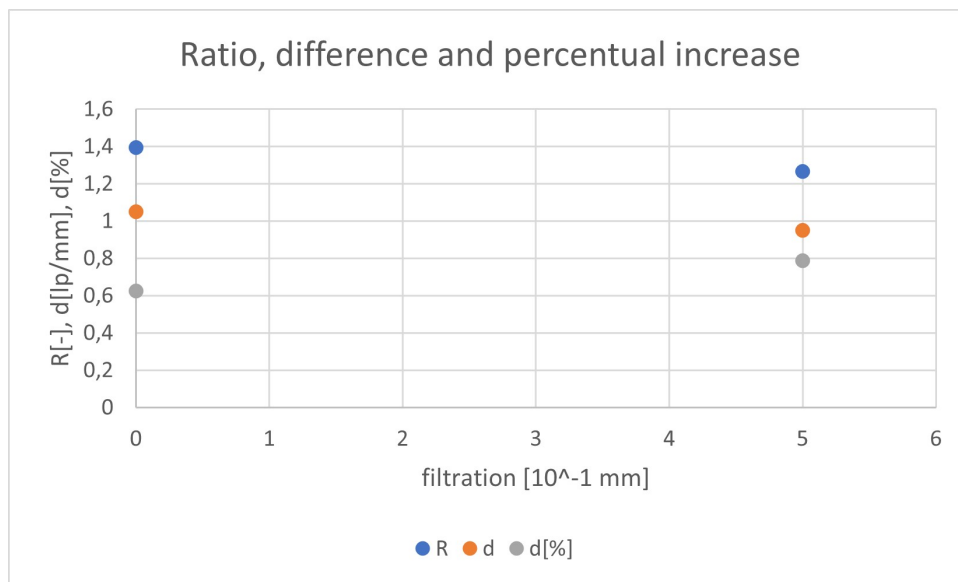


Figure 7.21: Ratio between 1 and 1.5 cm regions, difference between 1 and 1.5 cm regions, and percentile increase of $f(0.05)$ passing from 1.5 cm region to 1 cm region, without and with filtration respectively

Chapter 8

Conclusions

this chapter reports conclusions of the work, commenting results and presenting limitations and possible developments.

8.1 Results

After the characterization of the system 5, two methods of X ray tube performance analysis were presented 6, discussing the best way to implement them and discussing the intrinsic limitations. The Ratio method characterized by a fast implementation, without penalizing the reliability. It requires a reference standard for comparison. The optimal magnification method is also an accurate method of evaluation of the tube performance, it takes longer time to be performed, but it provides additional useful insights, such as optimal positioning of an object to be inspected or equivalent MTF expected imaging large objects.

Then, the optimal magnification method was used to analyse the effect of pre-filtration on equivalent focal spot, namely the one observed by the detector at the end of the source plus object system. The focal spot shows enlargement and this effect can explain the difference between pre and post filtration effect. Lastly, in 7, effect of filtration at source and tube is analysed, once again using MTF measures, in different situations, such as Water of different thicknesses in different positions, different thicknesses of iron and same spectrum compared to different materials with different thicknesses. Lastly, effect of filtration of object with different projected thickness is analysed, showing that filter can improve the overall performance of the system in terms of MTF.

8.2 Possible improvements

The main limitations of this work are connected to position measuring, due to difficulties in acquiring accurate measures by hand inside the cabinet. Providing accuracy to the centimetre, it is possible to create accurate maps of MTF(M), producing a more precise and accurate estimate of FS dimension. It

is possible to increase test numbers to increase statistics and provide a better esteem of uncertainty linked to the system.

Another interesting feature is to use the edge method to measure MTF, so that curves has not to be interpolating functions, but can be obtained by differentiation using the whole data acquired, eliminating convergence problems associated to the polynomial form of them.

8.3 Further developments

This thesis can be used as starting point for different works. The most important ones can probably be the study of the difference in MTF gain between pre-filtration and scattering grid. It was planned to do so, but due to technical reasons, grids were not available. Another important effort can be the dedicated to transfer these results directly to tomography. Lastly, the analysis of additional materials, both for objects and filters and their couples, can be explored to understand the maximum gain provided case-by-case. It can be of interest is a client has a main material to be analysed.

Bibliography

- [1] ASTM E2737-10, *Standard Practice for Digital Detector Array Performance Evaluation and Long-Term Stability*, ASTM International, West Conshohocken, PA, 2010
- [2] Bushberg Jerrold T., *The Essential Physics of Medical Imaging*, Philadelphia, LIPPINCOTT WILLIAMS & WILKINS, 2012
- [3] Paolo Russo, *Handbook of X-ray Imaging. Physics and Technology*, Naples, Italy, Taylor & Francis Group, 2018
- [4] Krzysztof Iniewski, *MEDICAL IMAGING. Principles, Detectors, and Electronics*, Hoboken, New Jersey, John Wiley & Sons, 2009
- [5] Carmignato S., Dewulf W. & Leach R., *Industrial X-Ray Computed Tomography*, s.l., Springer, 2018
- [6] J. Rueckel, M. Stockmar, F. Pfeiffer, J. Herzen, *State of the Art of CT Detectors and Sources: A Literature Review*, Published online, Springer, 1 February 2013
- [7] Ehsan Samei, *Advances in Digital Radiography: RSNA Categorical Course in Diagnostic Radiology Physics*, Duke University Medical Center, Durham, RSNA '03, 2003, pp 37-47.
- [8] P. Muller, J. Hiller, Y. Dai, J.L. Andreasen, H.N. Hansen, L. De Chiffre, *Estimation of measurement uncertainties in X-ray computed tomography metrology using the substitution method*, Published online, Elsevier CIRP Journal of Manufacturing Science and Technology, 24 May 2014
- [9] A. Webb, *Introduction to biomedical imaging* Hoboken, New Jersey, John Wiley & Sons, Inc., 2003 pp, 220-225
- [10] ASTM E1411-09, *Standard Practice for Qualification of Radioscopic Systems*, ASTM International, West Conshohocken, PA, 2009
- [11] ASTM E1647-09, *Standard Practice for Determining Contrast Sensitivity in Radiology*, ASTM International, West Conshohocken, PA, 2009
- [12] ASTM E2002-98, *Standard Practice for Determining Total Image Unsharpness in Radiology*, ASTM International, West Conshohocken, PA, 2009

- [13] M. Zahangir Kabir, Safa Kasap, *Springer Handbook of Electronic and Photonic Materials*, s.l., Springer, 2017
- [14] A. Rodr iguez-Sanchez, A. Thompson, L. Korner, N. Brierley, R. Leach, *Review of the influence of noise in X-ray computed tomography measurement uncertainty*, Published online, Elsevier Precision Engineering, 18 August 2020
- [15] J.Rueckel, M.Stockmar, F.Pfeiffer, J.Herzen, *Spatial resolution characterization of a X-ray microCT system*, Published online, Elsevier Applied Radiation and Isotopes ,30 August 2014
- [16] Erdi YE., *Computed tomography x-ray tube life analysis: a multiyear study*, Radiol Technol, 2013 Jul-Aug;84(6):567-70. PMID: 23861516.
- [17] M. R. Ay and A. Ahmadian, A. Maleki, H. Ghadiri, P. Ghafarian, H. Zaidi, *The Influence of X-ray Spectra Filtration on Image Quality and Patient Dose in the GE VCT 64-Slice Cardiac CT Scanner*, IEEE, s.l., 978-1-4244-2902-8/09/2009

Appendix A

MTF value equivalence

In the thesis was exploited the hypothesis that we could select any values of MTF as reference to our evaluations. However, this has to be proven.

Analysing the behaviour of the spatial frequencies for different values of MTF, it can be seen that the respective values at different mA give the same order for the points.

There are two considerations to be specified in order to give this statement rightfulness. The first one is of great concern for the validity of our assumption. In the curve named "f0.05", the point at 0.8 mA seems to have a different behaviour than the other curves. This is not a result of a physical problem but of the interpolation. In fact, the MTF curves obtained this way are interpolations, and their adherence to observation depends on what area of the curve are we interested in. Since the highest number of points are far from the value of 5%, this can be subjected to interpolation limitations. In fact, the values of 0.05 cannot be reached by the Excel Solver, due to the interpolating functional form. Thus, this point has no meaning in the evaluation.

The second consideration concern the points at higher mA. The validity of our assumption is preserved, but the decreasing behaviour has to be explained. It is a direct consequence of saturation of the FPD, and so in this operative conditions it is required to stay below these values to avoid such a disturbing effect.

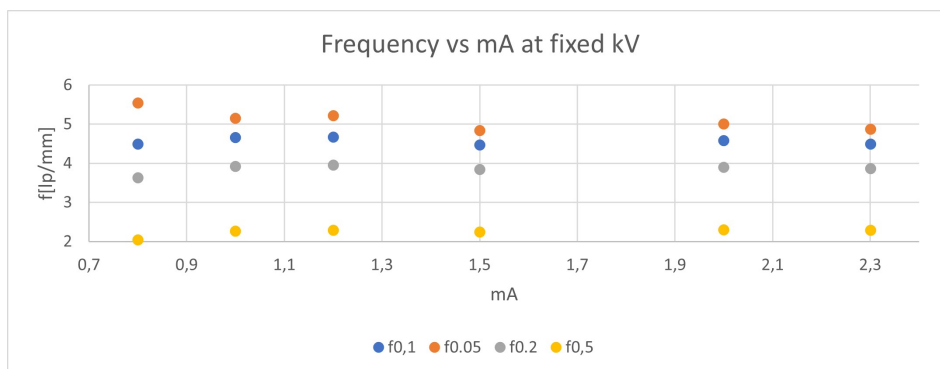


Figure A.1: Behavior of spatial frequencies for given MTF values at different mA, fixed kV

Appendix B

Matlab code for automatizing of Lag computation

```
L_IMG_1 = imread('acquisizioni Lag quatr _0000.tif ');
L_IMG_REF_OFF = imread('Riferimento X spenti.tif ');
L_IMGS0 = imread('acquisizioni Lag quatr _0000.tif ');
L_IMGS1 = imread('acquisizioni Lag quatr _0001.tif ');
L_IMGS2 = imread('acquisizioni Lag quatr _0002.tif ');

%%calcolo la ROI
somma_ROI_guess=0;
somma_ROI_ref=0;
counter=0;
i=0;
j=0;
for i=1:4087
    for j= 1:4047
        for x=i:i+9
            for y=j:j+49
                somma_ROI_guess = somma_ROI_guess + double(L_IMGS1(x,y));
                somma_ROI_ref = somma_ROI_ref + double(L_IMG_1(x,y));
            end
        end
    end
    val_ROI = (somma_ROI_guess)/somma_ROI_ref*100;
    savior(i,j)=val_ROI;
    if val_ROI==85
        counter=counter+1;
        roi=[i,j;i+9,j+49];
        for a = 1:2
            for b = 1:2
                ROI(a,b,counter)=roi(a,b);
            end
        end
    end
end
```

```

        end
    end
    fprintf('the selected ROI has rows from %d to %d and columns from %d to %d\n', i, i+49, j, j+9);
end

somma_ROI_guess=0;
somma_ROI_ref=0;
end
end
for i=1:4047
    for j=1:4087
        for x=i:i+49
            for y=j:j+9
                somma_ROI_guess = somma_ROI_guess + double(L_IMGS1(x,y));
                somma_ROI_ref = somma_ROI_ref + double(L_IMG_1(x,y));
            end
        end
        val_ROI = (somma_ROI_guess)/somma_ROI_ref*100;
        if val_ROI==85
            counter=counter+1;
            roi=[i , j ; i+49, j+9];
            for a = 1:2
                for b = 1:2
                    ROI(a,b,counter)=roi(a,b);
                end
            end
            fprintf('the selected ROI has rows from %d to %d and columns from %d to %d\n', i, i+49, j, j+9);
        end

somma_ROI_guess=0;
somma_ROI_ref=0;
end
end
GVS2mean=0;
GVoffmean=0;
GVonmean=0;
LAG4=0;
if counter>1
    for zz= 1:counter
        for xx= ROI(1,1,zz):ROI(2,1,zz)
            for yy = ROI(1,2,zz):ROI(2,2,zz)
                GVS2mean = GVS2mean + double(L_IMGS2(xx,yy))/500;
                GVoffmean = GVoffmean + double(L_IMG_REF_OFF(xx,yy))/500;
                GVonmean = GVonmean + double(L_IMG_1(xx,yy))/500;
            end
        end
    end
end

```

```
        end
    end
    LAG4(zz)=(GVS2mean-GVoffmean)/(GVonmean-GVoffmean)*100;
    end
    LAG4
    else
        fprintf('ROI not found\n');
    end
```